Development 140, 2597-2610 (2013) doi:10.1242/dev.087890
© 2013. Published by The Company of Biologists Ltd

Specification of chondrocytes and cartilage tissues from embryonic stem cells

April M. Craft[1], Nazish Ahmed[2], Jason S. Rockel[3], Gurpreet S. Baht[3], Benjamin A. Alman[3], Rita A. Kandel[2], Agamemnon E. Grigoriadis[4] and Gordon M. Keller[1,*]

SUMMARY

Osteoarthritis primarily affects the articular cartilage of synovial joints. Cell and/or cartilage replacement is a promising therapy, provided there is access to appropriate tissue and sufficient numbers of articular chondrocytes. Embryonic stem cells (ESCs) represent a potentially unlimited source of chondrocytes and tissues as they can generate a broad spectrum of cell types under appropriate conditions *in vitro*. Here, we demonstrate that mouse ESC-derived chondrogenic mesoderm arises from a Flk-1^{-}/Pdgfrα^{+} (F^{-}P^{+}) population that emerges in a defined temporal pattern following the development of an early cardiogenic F^{-}P^{+} population. Specification of the late-arising F^{-}P^{+} population with BMP4 generated a highly enriched population of chondrocytes expressing genes associated with growth plate hypertrophic chondrocytes. By contrast, specification with Gdf5, together with inhibition of hedgehog and BMP signaling pathways, generated a population of non-hypertrophic chondrocytes that displayed properties of articular chondrocytes. The two chondrocyte populations retained their hypertrophic and non-hypertrophic properties when induced to generate spatially organized proteoglycan-rich cartilage-like tissue *in vitro*. Transplantation of either type of chondrocyte, or tissue generated from them, into immunodeficient recipients resulted in the development of cartilage tissue and bone within an 8-week period. Significant ossification was not observed when the tissue was transplanted into osteoblast-depleted mice or into diffusion chambers that prevent vascularization. Thus, through stage-specific manipulation of appropriate signaling pathways it is possible to efficiently and reproducibly derive hypertrophic and non-hypertrophic chondrocyte populations from mouse ESCs that are able to generate distinct cartilage-like tissue *in vitro* and maintain a cartilage tissue phenotype within an avascular and/or osteoblast-free niche *in vivo*.

KEY WORDS: Cartilage, Chondrocyte, Embryonic stem cell, Induced pluripotent stem cell, Paraxial, Somite

INTRODUCTION

The ability to efficiently and reproducibly generate differentiated cell types from pluripotent stem cells *in vitro* has opened the door for the development of cell-based therapies for the treatment of a broad range of degenerative and debilitating diseases. Osteoarthritis (OA) is a candidate for such therapy as it affects at least one in ten adults (Lawrence et al., 2008), leaving patients with a poor quality of life due to pain associated with joint movement. Pathogenic hallmarks of OA include the degradation of the extracellular matrix (ECM) of articular cartilage, which lines the joints, together with thickening of the underlying subchondral bone and the formation of osteophytes (bone spurs). Articular cartilage is generated by a distinct subpopulation of chondrocytes known as articular chondrocytes (ACs) that are specified early in development and persist throughout adult life. Although ACs function to maintain integrity of the articular cartilage under normal circumstances, they display little capacity to repair cartilage damaged by injury or disease. Consequently, with disease progression, damage to the cartilage is so extensive that surgical intervention, such as joint replacement, is often required to improve the quality of life for the patient. ACs differ from growth plate chondrocytes (GPCs), the primary function of which is to provide a cartilage template on which new bone can form through the process of endochondral ossification (Colnot, 2005). During this process, GPCs undergo hypertrophy and die, providing a cartilage scaffold for the formation of bone. Although normal healthy ACs are not hypertrophic, they can display some characteristics of GPCs, including hypertrophy, with the onset of OA. This transition to a hypertrophic phenotype might contribute to the pathogenesis of this disease.

Chondrocyte and cartilage replacement represent a potential new therapy for OA that could, at some point dramatically reduce the need for mechanical devices. This type of therapy, however, is dependent on access to appropriate tissue and sufficient numbers of highly enriched ACs. It is well established that adult mesenchymal stem cells (MSCs) are able to differentiate to chondrocytes *in vitro*; however, it is unclear whether they are able to give rise to ACs as the cartilage-like tissue generated from them undergoes hypertrophy prematurely (Pelttari et al., 2008; Pelttari et al., 2006; Steinert et al., 2007). Alternatively, ACs have been harvested directly from patients and used for tissue generation *ex vivo*, despite their limited capacity to proliferate. Tissue generated by passaged chondrocytes exhibits fibrocartilage characteristics and can improve the quality of life for the patient in the short term but ultimately undergoes degradation as it lacks sufficient weight-bearing capacity (LaPrade et al., 2008; Tins et al., 2005). Pluripotent stem cells (PSCs) [embryonic stem cells (ESCs) and induced pluripotent stem cells (iPSCs)] represent a novel and potentially unlimited source of chondrocytes and tissues for therapeutic applications as these cells are able to generate a broad spectrum of cell types under appropriate conditions *in vitro*. As with all other cell types derived from PSCs, the efficient and reproducible generation of ACs from PSCs will

[1]McEwen Centre for Regenerative Medicine, University Health Network, Toronto, ON, M5G 1L7, Canada. [2]CIHR-BioEngineering of Skeletal Tissues Team, Mount Sinai Hospital, University of Toronto, ON, M5G 1X5, Canada. [3]Developmental and Stem Cell Biology, Hospital for Sick Children, Toronto, ON, M5G 1L7, Canada. [4]Department of Craniofacial Development and Stem Cell Biology, Guy's Hospital, King's College London, London, SE1 9RT, UK.

*Author for correspondence (gkeller@uhnresearch.ca)

Accepted 22 April 2013

depend on our ability to recapitulate key aspects of embryonic development *in vitro*.

Chondrocytes in the vertebrae and ribs develop from paraxial mesoderm, whereas chondrocytes in the long bones and most of the girdles are derived from lateral plate mesoderm (LPM), which also gives rise to hematopoietic and cardiovascular lineages (Kinder et al., 1999; Lawson et al., 1991). Following induction, strips of paraxial mesoderm are segmented into somites (Kulesa and Fraser, 2002; Tam and Tan, 1992). Somite development is regulated, in part, by the transcription factors paraxis (Tcf15) and Tbx18, the expression of which coincides with the induction of paraxial mesoderm (Burgess et al., 1996; Bussen et al., 2004; Singh et al., 2005). Individual somites are then patterned into the ventral sclerotome, which forms the axial skeleton, including cartilage and the vertebral column, and the dorsal dermomyotome which develops into skeletal muscles and the dermis of the back (Hirsinger et al., 2000). Specification of the sclerotome is marked by the expression of two transcription factors, Meox1 (Mankoo et al., 2003) and Nkx3.2 (also known as Bapx1). A population of collagen 2 (Col2a1)-positive mesenchymal cells with chondrogenic potential develops from sclerotome-derived cells at embryonic day (E) 12.5 of mouse development (Akiyama et al., 2002; Dao et al., 2012).

Whereas methods for differentiating progenitor cells to the chondrogenic lineage are well established, the ability to specify ACs, and ultimately articular cartilage tissue, remains poorly understood. ACs are derived from interzone cells, a fibrotic population of cells that forms at future sites of synovial joints, marked by the upregulation of Wnt9a (previously known as Wnt14) and growth and differentiation factor 5 (Gdf5; previously known as BMP14 in human), a member of the TGFβ superfamily (Archer et al., 2003; Pacifici et al., 2006). Lineage-tracing studies have shown that Gdf5-expressing interzone cells give rise to several joint tissues, including ACs, but do not contribute to the GPC population (Koyama et al., 2008). GPCs, by contrast, develop from the condensing chondrogenic mesenchyme and express Bmp2, Bmp4 and Bmp7, as well as hypertrophy-related genes, including collagen 10. Distinct regions of ACs and GPCs are observed as early as postnatal day 7-8 when the secondary ossification center begins to form (Blumer et al., 2007; Murakami et al., 2004). These observations suggest that ACs and GPCs are generated from separate progenitor populations during development and, as such, might represent distinct lineages.

A number of studies have demonstrated that it is possible to derive chondrocytes from mouse (m) and human ESCs and iPSCs *in vitro*. Most, however, used serum-based media to support the early stages of differentiation, resulting in the generation of mixed lineage end-stage cultures (Hwang et al., 2006; Hwang et al., 2008; Jukes et al., 2008; Kramer et al., 2000; Yamashita et al., 2008; zur Nieden et al., 2005). Recent studies have reported the use of defined culture media with specific pathway agonists and antagonists to direct differentiation and in doing so have provided insights into the regulation of paraxial mesoderm and chondrocyte development (Darabi et al., 2008; Nakayama et al., 2003; Tanaka et al., 2009). In one of the most detailed studies with mESCs, Tanaka et al. (Tanaka et al., 2009) showed that the combination of Wnt signaling with bone morphogenetic protein (BMP) inhibition resulted in the generation of paraxial mesoderm with chondrogenic potential, identified by the expression of Pdgfrα and a lack of expression of Flk-1 (Kdr – Mouse Genome Informatics). This mesoderm also displayed some cardiac potential but showed no capacity to generate hematopoietic cells, indicating that dependency on BMP signaling distinguishes different types of mesoderm.

In this study, we have traced the origin of the chondrogenic lineage from mESCs and demonstrate that it arises from a Flk-1^{-}/Pdgfrα^{+} (F^{-}P^{+}) mesoderm population that emerges following the development of an early cardiogenic F^{-}P^{+} population. Specification of this chondrogenic mesoderm with either BMP4 or the combination of Gdf5, cyclopamine and soluble Bmpr1α (sBmpr1α) resulted in the development of populations with hypertrophic and non-hypertrophic chondrocyte characteristics, respectively. These chondrocyte populations formed spatially organized, proteoglycan-rich tissue *in vitro* and retained their hypertrophic and non-hypertrophic phenotype during this process. Transplantation of either type of chondrocyte or tissues generated from them into immunodeficient recipients resulted in the development of cartilage tissue and bone within an 8-week period. Ossification was dramatically reduced or completely absent in tissue transplanted into osteoblast-depleted mice or in diffusion chambers that prevented host vascularization. Together, these findings demonstrate that through stage-specific manipulation of appropriate signaling pathways it is possible to efficiently and reproducibly generate chondrogenic mesoderm that can be specified into populations with hypertrophic and non-hypertrophic chondrocyte properties.

MATERIALS AND METHODS

ESC maintenance and differentiation

GFP-Bry (Fehling et al., 2003) mESCs, T-EGFP/*Rosa26*-tdRFP (RFP.bry) (Luche et al., 2007) mESCs and Oct4-GFP miPSCs (Stadtfeld et al., 2008) were maintained in a modified serum-free (SF), feeder-free culture system as described previously (Gadue et al., 2006; Ying et al., 2003). For differentiation, ESCs were dissociated and cultured in suspension in serum-free differentiation medium (SFD) (Gouon-Evans et al., 2006) without additional growth factors for 48 hours. Embryoid bodies (EBs) were then dissociated and re-aggregated in SFD with the addition of growth factors or inhibitors as indicated [9 ng/ml activin A (inhibin, beta A), 25 ng/ml Wnt3a, 5 ng/ml vascular endothelial growth factor (VEGF), 150 ng/ml noggin, 0.5 ng/ml BMP4]. EBs were harvested 24 hours later, the cells dissociated and the appropriate populations isolated by cell sorting. For re-aggregation, sorted cells were cultured at 250,000 cells/ml in 24-well ULA dishes (Costar) for 48 hours in SFD containing 10 ng/ml bFGF (FGF2) and 10 μM Y-27632. Aggregates were harvested and dissociated to single-cell suspension, and appropriate populations were isolated by cell sorting, if applicable. Cells were cultured in monolayer on 0.1% gelatin-coated 96-well tissue culture dishes (Falcon, Becton Dickinson) at 30,000-120,000 cells/ml in SFD containing 2 mM L-glutamine, 10 ng/ml bFGF, and the following, as indicated: 30-100 ng/ml BMP4, 30 ng/ml Gdf5, 0.25 uM KAAD-cyclopamine, 500 ng/ml sBmpr1α, 2-4 μM dorsomorphin (Sigma). Human activin A, BMP4, VEGF, bFGF and noggin, mouse Wnt3a and Gdf5, and sBmpr1α were purchased from R&D Systems; Y-27632 and KAAD-cyclopamine were obtained from Toronto Research Chemicals.

Flow cytometry and cell sorting

EBs generated from mESC differentiation experiments were dissociated by incubation with TrypLE (Invitrogen) and stained with following antibodies: anti-mouse Flk-1-biotin, anti-mouse Pdgfrα (CD140a)-allophycocyanin (APC; clone APA5, eBioscience, San Diego, CA, USA), streptavidin-phycoerythrin (PE) or streptavidin-PE-Cy7 (BD Pharmingen). Most antibody stains were performed at 4°C in PBS containing 5% (v/v) fetal calf serum (FCS). For cell sorting, antibody stains were performed in Iscove's modified Dulbecco's medium (IMDM) containing 0.2% BSA (Sigma). Cells were acquired using a LSR II flow cytometer (Becton Dickinson) or sorted using a FACS ARIA II (Becton Dickinson). Analysis was performed using FlowJo (Tree Star).

Quantitative real-time PCR

Total RNA was prepared with the RNAqueous-Micro Kit (Ambion) with DNase treatment. RNA (0.1-1 μg) was reverse transcribed using random

hexamers and oligo(dT) with Superscript III reverse transcriptase (Invitrogen). Real-time quantitative (Q)-PCR was performed on a MasterCycler EP RealPlex (Eppendorf) using Quantifast SYBR Green (Qiagen). Genomic DNA standards were used to evaluate the efficiency of the PCR and to calculate the copy number of each gene relative to the housekeeping gene *Actb*. Mean and standard errors of three to six independent experiments were calculated. Student's *t*-test was used to evaluate statistical significance. Oligonucleotide sequences are listed in supplementary material Table S1.

Alcian Blue staining and fluorescence microscopy

Monolayer cultures were fixed in 4% paraformaldehyde. For Alcian Blue staining, monolayers were washed in 0.5 N HCl, then stained with 0.25% (w/v) Alcian Blue 8GX (Sigma) in 0.5 N HCl overnight. Cultures were visualized by microscopy or imaged using a Scanmaker i900 Microtek scanner. Alcian Blue dye was solubilized overnight in 8 M guanidine hydrochloride (Sigma) and quantified by absorbance at 595 nm using a spectrophotometer. For immunofluorescence, monolayer cultures were stained using an antibody against the cardiac isoform of troponin T (cTnT) (clone 13-11, NeoMarkers, Fremont, CA, USA) and a donkey anti-mouse Alexa488-conjugated secondary antibody (Invitrogen). Cultures were counterstained with DAPI (Dako).

In vitro tissue formation

Monolayer cultures derived in indicated conditions for 12 days were treated with 0.2% (w/v) collagenase (Sigma), followed by brief trypsinization to obtain a single-cell suspension. Cells (1.5×10^6) were seeded onto type II collagen-coated Millicell culture plate inserts (60 mm^2; Millipore, Bedford, MA, USA). Cultures were maintained in Dulbecco's modified Eagle's medium (DMEM) (containing 20% FBS, high glucose) for 2-5 weeks (Ahmed et al., 2009).

Cell injections and tissue transplantations

Monolayer cultures were dissociated and cells were resuspended in growth factor-reduced matrigel (Becton Dickinson). Cells (500,000) were injected in a volume of 30 μl subcutaneously near the mammary fat pad of B10;B6-*Rag2*^{tm1Fwa} *Il2rg*^{tm1Wjl} female mice aged 4-6 weeks. Alternatively, biopsy punches of cartilage-like tissues (4 mm diameter; derived from either day 5 unsorted GFP-Bry mESCs or Pdgfrα$^+$ cells sorted from RFP.bry mESCs) were transplanted subcutaneously between the shoulder blades. Cartilage-like tissues were placed within diffusion chambers (Millipore) and transplanted subcutaneously in B10;B6-*Rag2*^{tm1Fwa} *Il2rg*^{tm1Wjl} female mice aged 4-6 weeks. Grafts were harvested as indicated.

DTK mice carry a herpes simplex virus thymidine kinase gene under control of the osteoblast-specific 2.3-kb fragment of the rat collagen α1 type I promoter (Dacquin et al., 2002; Visnjic et al., 2001). Upon treatment with gancyclovir (6.25 mg/kg/day) endogenous osteoblasts of DTK mice undergo ablation (Ng et al., 2011). Mice either lacking (DTK$^-$) or carrying (DTK$^+$) the DTK transgene were injected with mESC-derived chondrocytes subcutaneously at the mammary fat pad site as described above at 12-16 weeks of age. All mice were treated with gancyclovir (Sigma) for an 8-week period, at which point the engraftments were harvested.

Histology and Immunohistochemistry

In vitro-derived cartilage-like tissues, and engraftments from *in vivo* studies were fixed in 10% formalin and embedded in paraffin. Five-micron-thick sections were stained with Toluidine Blue, Hematoxylin and Eosin (H&E), Safranin O, and von Kossa, as indicated. Immunohistochemical analysis was performed using antibodies recognizing collagen type 2 (MS306-P, Labvision, Fremont, CA, USA), collagen 10 (X53; Quartett, Berlin, Germany) and red fluorescent protein (Abcam). Sections were counterstained with Mayer's Hematoxylin.

RESULTS

Induction of chondrogenic mesoderm

In order to generate chondrogenic mesoderm efficiently from mESCs, we used a protocol in which a primitive streak (PS)-like population is formed and mesoderm is induced within a 24-hour period between days 2 and 3 of differentiation by a combination of activin/nodal, Wnt and BMP signaling (Nostro et al., 2008). In these studies, activin/nodal signaling is initiated by the addition of activin A (activin) whereas BMP signaling is manipulated by the presence or absence of the agonist BMP4 or the inhibitor noggin. We used the GFP-Bry mESC reporter cell line in order to monitor PS/early mesoderm formation and to isolate populations by flow cytometry based on GFP expression (Fehling et al., 2003) (Fig. 1A). The Oct4-GFP mouse iPSC line (Stadtfeld et al., 2008) was included to demonstrate the applicability of this protocol for miPSC differentiation (supplementary material Fig. S1).

Day 3 embryoid bodies (EBs) induced in the absence of BMP signaling (no BMP4 or noggin) in the presence of activin, Wnt and VEGF contained 80-85% GFP-Bry$^+$ cells, demonstrating efficient PS/mesoderm formation under these conditions. The addition of BMP4 during the induction stage led to a modest increase in the proportion of GFP-Bry$^+$ cells to >90%. Although GFP-Bry PS-like populations were efficiently generated with the three conditions, the size of the specific mesoderm subsets, defined by the expression profiles of the cell surface receptors Flk-1 (F) and Pdgfrα (P), differed dramatically between the BMP4-induced and noggin-induced EBs in both mESC and miPSC cultures (Fig. 1B; supplementary material Fig. S1C). With this combination of markers, the F$^+$P$^-$ population represents hemangioblast/hematopoietic mesoderm, the F$^+$P$^+$ population cardiogenic mesoderm, and the F$^-$P$^+$ population chondrogenic mesoderm (Kattman et al., 2011; Takakura et al., 1997). BMP4-induced EBs contained a large F$^+$P$^+$ population, and substantially smaller F$^-$P$^+$ and F$^-$P$^-$ populations. These EBs also contained a small, but detectable F$^+$P$^-$ population. By contrast, EBs differentiated in the absence of BMP signaling had no detectable F$^+$P$^-$ population, a dramatically smaller F$^+$P$^+$ population and larger F$^-$P$^+$ and F$^-$P$^-$ populations than those induced with the agonist (Fig. 1B). Following induction, EBs were dissociated and cells were re-aggregated in the presence of bFGF for 2 days (day 5 of differentiation) to specify a chondrogenic fate (Fletcher and Harland, 2008) (Fig. 1A).

Gene expression analyses of day 2 and day 3 EBs, and the day 5 aggregates revealed distinct differences in the populations induced in the presence or absence of BMP4 (Fig. 1C,D). Cells induced with BMP4 expressed significantly higher levels of genes associated with LPM [*Mesp1*, *Foxf1a* (*Foxf1* – Mouse Genome Informatics)] (Ormestad et al., 2004) hematopoietic (*Gata1*) and cardiac (*Nkx2.5*) development compared with those generated in the absence of BMP signaling (Fig. 1C). Expression of *Mesp1* was restricted to the day 3 BMP4-induced EBs whereas *Foxf1a* was detected in both the day 3 EBs and day 5 aggregates. *Gata1* was expressed only in the day 5 aggregates derived from BMP4-induced EBs, suggesting that hematopoietic potential was restricted to this population. Methylcellulose-based colony assays confirmed the molecular studies and showed that primitive erythroid and macrophage progenitors were detected only in BMP4-induced EBs (supplementary material Fig. S2). *Nkx2.5* was expressed in BMP4-induced cultures on day 3 and on day 5, and at levels that were significantly higher than those in comparable EBs and aggregates generated in the absence of BMP signaling.

In contrast to the expression of LPM-associated transcription factors, genes indicative of paraxial mesoderm and somite development, including *Tcf15*, *Meox1*, *Nkx3.2* and *Tbx18* were expressed at significantly higher levels in the day 5 aggregates derived from EBs induced in the absence of BMP signaling (Fig. 1D). Gene expression analyses of day 5 aggregates from

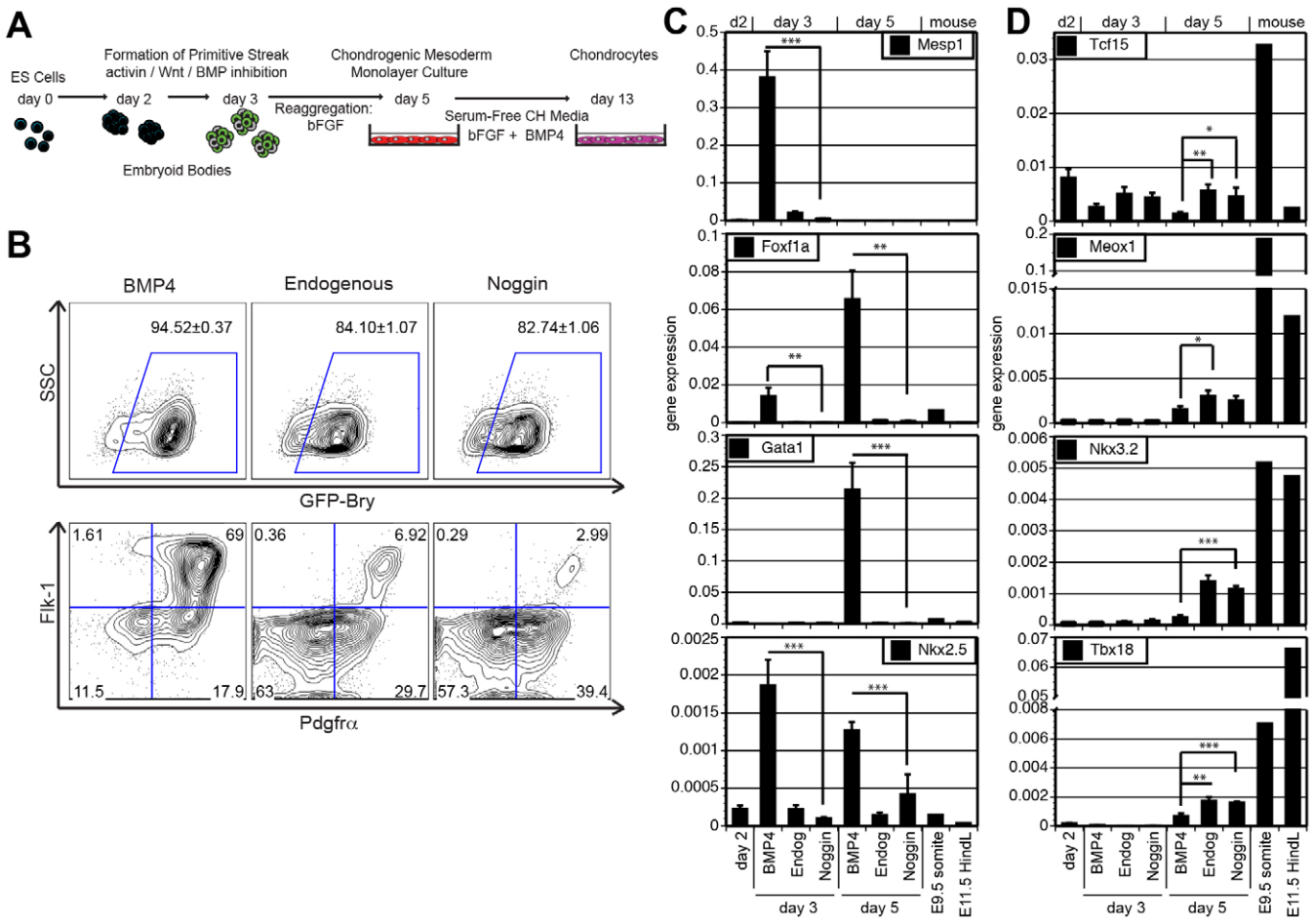

Fig. 1. BMP signaling influences mesoderm development from mESCs. (**A**) Protocol for induction and specification of chondrogenic mesoderm from mESCs. GFP-Bry mESCs were induced at day 2 for 24 hours with activin, Wnt3a, VEGF, and one of the following: BMP4, no BMP4 (Endogenous, Endog), or noggin. On day 3 of culture, EBs were re-aggregated in the presence of bFGF for 2 days and then plated in monolayer culture in SFD containing BMP4 and bFGF for up to 12 days. (**B**) Flow cytometric analysis showing brachyury (GFP-Bry) induction and expression of Flk-1 and Pdgfrα on the GFP-Bry^{+} gated cells after 1 day induction in indicated conditions. (**C**,**D**) Q-PCR analysis of expression of (C) lateral plate mesoderm genes (*Mesp1* and *Foxf1a*), a hematopoietic transcription factor gene (*Gata1*) and a cardiac transcription factor gene (*Nkx2.5*), and (D) paraxial mesoderm (*Tcf15*) and somite (*Meox1*, *Nkx3.2*, *Tbx18*) genes in day 2 EBs, day 3 EBs and day 5 aggregates. Values represent copy number relative to β-actin and compared with mouse embryonic tissues, E9.5 somites and E11.5 hindlimbs (HindL). Error bars indicate s.e.m. (n=5). *P<0.05, **P<0.01, ***P<0.001.

miPSC differentiations showed very similar patterns (supplementary material Fig. S1D,E). Taken together, these findings demonstrate that BMP is required for the generation of hematopoietic and cardiac mesoderm, whereas chondrogenic mesoderm that expresses markers associated with paraxial mesoderm and somites develops in the absence of the BMP signaling pathway. These results confirm previous results in our laboratory (Kattman et al., 2011; Nostro et al., 2008) and those of Tanaka et al. (Tanaka et al., 2009).

Specification of the chondrocyte lineage

Whereas inhibition of the BMP pathway promoted the development of chondrogenic mesoderm that displayed paraxial and somite gene expression patterns, activation of TGFβ signaling is required to specify the chondrocyte lineage (Kramer et al., 2000; zur Nieden et al., 2005). Therefore, to generate chondrocytes from the activin/Wnt-induced mesoderm, day 5 aggregates were dissociated and the cells plated in monolayer culture in SFD containing BMP4 and bFGF [chondrocyte (CH) media]. Analyses of the monolayer populations after 9 days revealed that *Sox9* and *Sox5*, genes encoding two transcription factors required for chondrocyte development, were expressed in cells generated from mesoderm induced in the absence of BMP4 (Fig. 2A). Cells derived from BMP4-induced EBs expressed significantly lower levels of these genes. Similarly, ECM genes collagen 2 (*Col2a1*) and aggrecan, indicative of chondrocyte maturation, were expressed at significantly higher levels in the endogenous and noggin-induced cultures compared with BMP4-induced cultures (Fig. 2B). Chondrocytes were easily identified in monolayer cultures derived from the untreated and noggin-induced cells (Fig. 2C; supplementary material Fig. S1F) after 8 days (day 13 of differentiation) by their cobblestone-like appearance and the production of ECM that stains positively with Alcian Blue (Fig. 2D). Chondrocytes did not develop in monolayers generated from BMP4-induced mesoderm. Taken together, these findings clearly indicate that mesoderm induced in the absence of BMP4 signaling contains significantly greater chondrogenic potential than the BMP4-induced mesoderm.

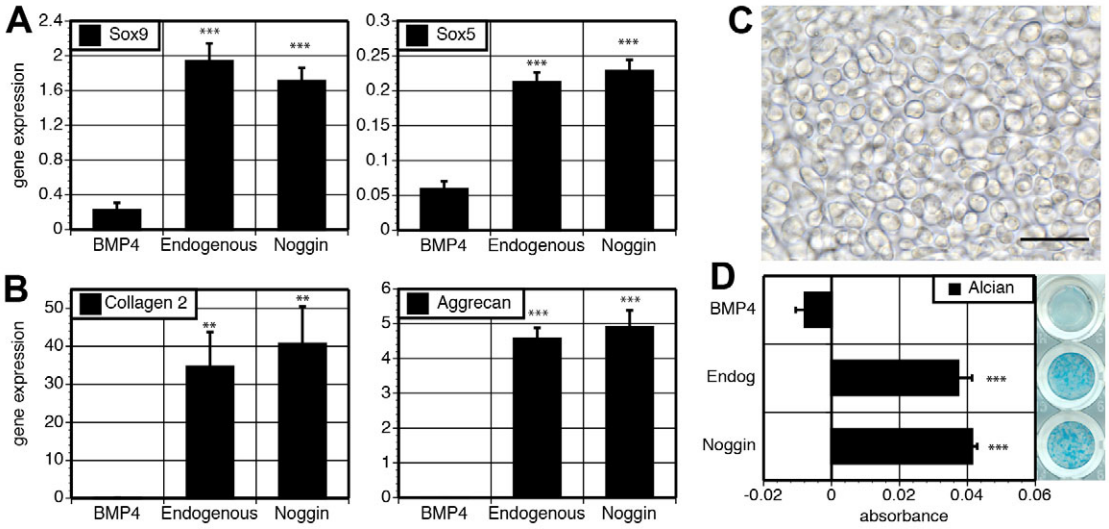

Fig. 2. Bmp4 signaling during primitive streak induction negatively regulates chondrogenic potential of mESCs. (**A**,**B**) Day 5 cells, induced as in Fig. 1A, were plated in monolayer culture in CH media for 9 days. Q-PCR analysis of (A) *Sox9* and *Sox5*, and (B) collagen 2 and aggrecan expression in end stage cultures. (**C**) Morphology of chondrocytes derived from noggin-induced cells. Scale bar: 50 μm. (**D**) End-stage cultures were stained with Alcian Blue (representative wells depicted) and Alcian Blue was quantified as described in the Materials and methods. Error bars indicate s.e.m. (n=3-6). Significance is compared with BMP4-induced cultures; $^{**}P<0.01$, $^{***}P<0.001$.

Temporal development of chondrogenic mesoderm

To define further the relationship of the cardiogenic and chondrogenic mesoderm lineages and to establish their temporal patterns of development, we analyzed day 3 Bry^+P^+ and Bry^+P^- mesoderm, and populations derived from them, for cardiomyocyte and chondrocyte potential (Fig. 3A). The Bry^+P^+ and Bry^+P^- fractions were isolated from day 3 EBs and the cells were re-aggregated for 2 days, as in previous studies. Analyses of day 5 aggregates revealed that the population derived from the day 3 Bry^+P^+ mesoderm had downregulated Pdgfrα (referred to as population 1 or P1) over the 2-day culture period. By contrast, day 3 Bry^+P^- mesoderm (P2) generated a new or second P^+ population during this time that had downregulated GFP-Bry expression (supplementary material Fig. S3). On day 5, the newly generated Bry^-P^+ fraction (designated P3, or the 'second wave' of Pdgfrα expression) as well as the day 5 Bry^-P^- fraction (designated P4) were isolated from the P2 aggregates (derived from day 3 Bry^+P^-) and their developmental potential was compared with the day 5 P1 population derived from 'first wave' Bry^+P^+ cells.

Nkx2.5 expression was detected only in the P1 population, indicating that cardiac potential was restricted to the early developing (day 3, P1) P^+ mesoderm (Fig. 3B). By contrast, expression of paraxial mesoderm/somite genes *Tcf15*, *Meox1*, *Nkx3.2* and *Tbx18* segregated to the later developing P^+ (P3) population (Fig. 3C-F). Further analyses of these populations confirmed that contracting cardiomyocytes that expressed cardiac troponin T (cTnT; Fig. 3G) developed from the P1 cells, as expected, but not from the P2 (Fig. 3H) or P3 cells (not shown). By contrast, chondrocytes displaying typical cobblestone-like appearance were observed in monolayer cultures derived from P3 cells (Fig. 3I), but not from the P1 cardiogenic fraction. Collectively, these findings demonstrate that cardiogenic and chondrogenic mesoderm develop as Pdgfrα-expressing populations in a defined temporal pattern in mESC differentiation cultures. The P^+ population that develops early (day 3) contains cardiac mesoderm, whereas the later developing P^+ cells (day 5) display chondrogenic mesoderm potential as defined by gene expression patterns and the capacity to generate chondrocytes.

Tracking the development of the Pdgfrα populations demonstrated the sequential specification of cardiac and chondrogenic mesoderm, and allowed us to isolate chondrogenic mesoderm from any remaining cardiac mesoderm. Based on the temporal patterns of mesoderm development provided by these studies, we were able to selectively isolate a population enriched in chondrogenic mesoderm by simply sorting the P^+ population from day 5 aggregates generated from day 3 activin/Wnt/noggin-induced EBs (non-fractionated) (Fig. 4A). This single sorted day 5 P^+ ($d5P^+$) population expressed higher levels of the somite genes *Tcf15*, *Meox1*, *Nkx3.2* and *Tbx18* than the day 5 P^- ($d5P^-$) fraction (Fig. 4B). When plated in monolayer culture in CH media, the $d5P^+$ cells differentiated to the chondrogenic lineage as demonstrated by the upregulation of *Sox9*, collagen 2, *Sox5* and aggrecan (Fig. 4C,D; supplementary material Fig. S4) and by the emergence of a highly enriched population of chondrocytes by day 11 of culture (Fig. 4E). Monolayers derived from $d5P^-$ cells also expressed these genes and gave rise to some chondrocytes. However, expression was delayed, and in most cases was significantly lower than the levels detected in the $d5P^+$-derived cells (Fig. 4C,D). Cultures derived from $d5P^-$ cells were not homogeneous, but rather consisted of mixed populations of chondrocytes and other cell types (Fig. 4F). Analysis of the $d5P^-$-derived monolayer cultures revealed the emergence of a P^+ population within 1 day of plating (not shown), suggesting that the chondrogenic potential of the $d5P^-$ cells develops through a P^+ intermediate and that the window of chondrogenic mesoderm induction, as defined by the upregulation of Pdgfrα, extends beyond day 5 of differentiation.

Hypertrophic and non-hypertrophic chondrocytes are generated from mESC-derived chondrogenic mesoderm

Access to different stages of mesoderm and chondrocyte development in the differentiation cultures provides a unique opportunity to investigate the pathways that specify the two

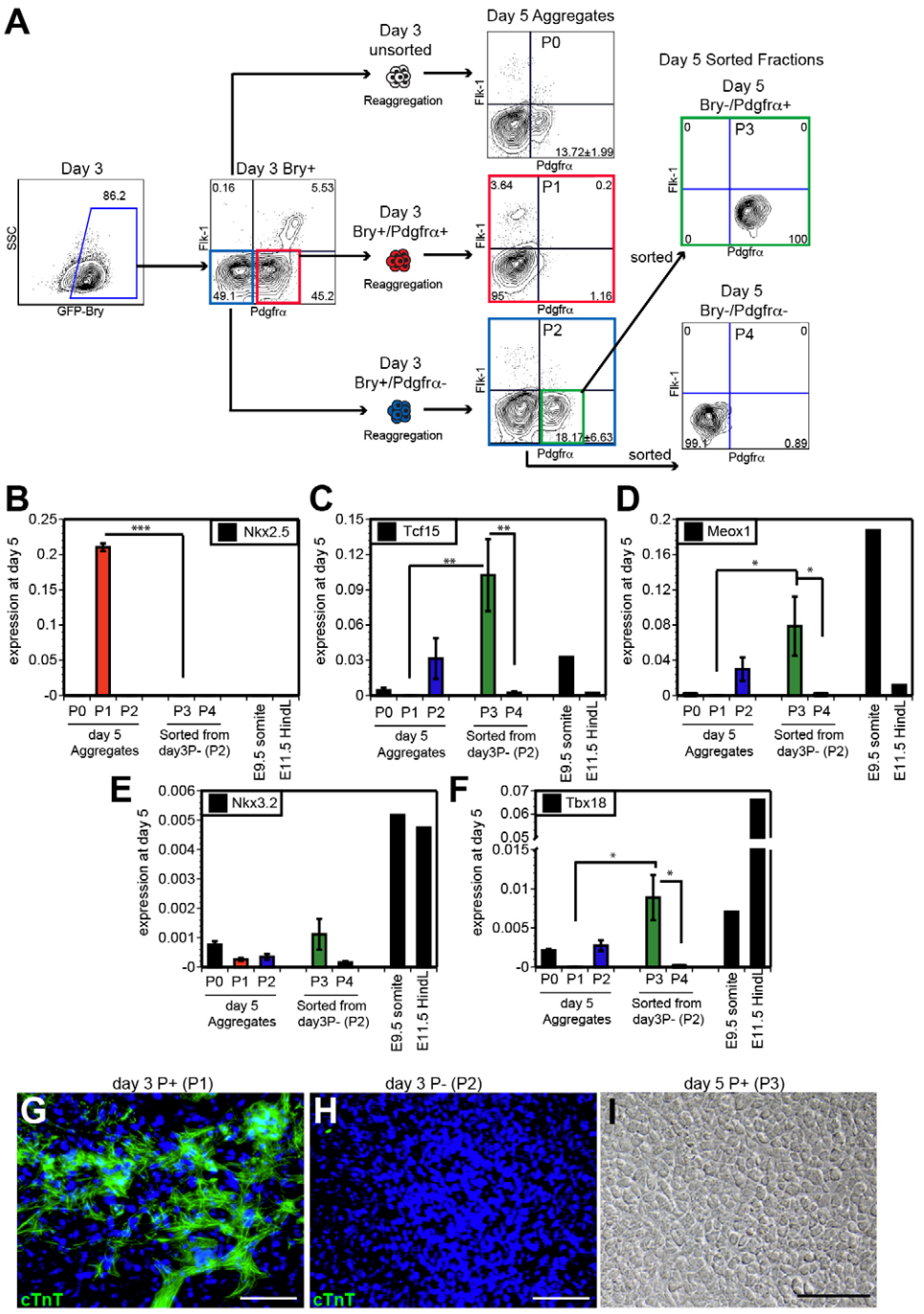

Fig. 3. Day 5 Pdgfrα$^+$ (P$^+$)-enriched population contains chondrogenic potential. (**A**) FACS analyses of noggin-induced cultures and sorted fractions on day 3 and day 5 of differentiation. Bry$^+$P$^+$ and Bry$^+$P$^-$ populations were sorted from day 3 cultures and aggregated for 2 days as in Fig. 1A. A Bry$^-$P$^+$ population exists in unsorted day 5 aggregates (P0). Day 3 Bry$^+$P$^+$ derived cells (P1, red) lost Pdgfrα expression by day 5, whereas a population of day 3 Bry$^+$P$^-$ cells upregulated expression of Pdgfrα by day 5 (P2, blue; *n*=4). P$^+$ cells were sorted from the day 5 P2 aggregates (P3, green). Day 5 P$^-$ cells sorted from the P2 aggregates were designated P4. (**B-F**) Q-PCR analysis of *Nkx2.5*, *Tcf15*, *Meox1*, *Nkx3.2* and *Tbx18* expression in day 5 aggregates from Bry$^+$ populations sorted based on Pdgfrα expression on day 3 (P0, P1, P2) and from P2 aggregates on day 5 (P3, P4) as indicated. HindL, hindlimbs. (**G**,**H**) Cardiac troponin T expression (cTnT, green) was detected by immunofluorescence in P1 cells (G) but not P2 cells (H) after monolayer culture; DAPI counterstain (blue). (**I**) Monolayer cultures derived from P3 sorted cells were highly enriched with chondrocytes. Scale bars: 100 μm. Error bars indicate s.e.m. (*n*=4). **P*<0.05, ***P*<0.01, ****P*<0.001.

different chondrocytes populations, ACs and GPCs, from PSCs. As a first step, we compared the effect of stimulating the cells during the 12-day monolayer culture with either BMP4 or Gdf5 (Fig. 5A). Monolayer cultures stimulated by the two agonists displayed distinct morphological differences. Those treated with BMP4 comprised a relatively homogeneous population of cells exhibiting a chondrocyte phenotype (Fig. 5B). By contrast, Gdf5-treated cultures had distinct colonies of chondrocytes separated by flat

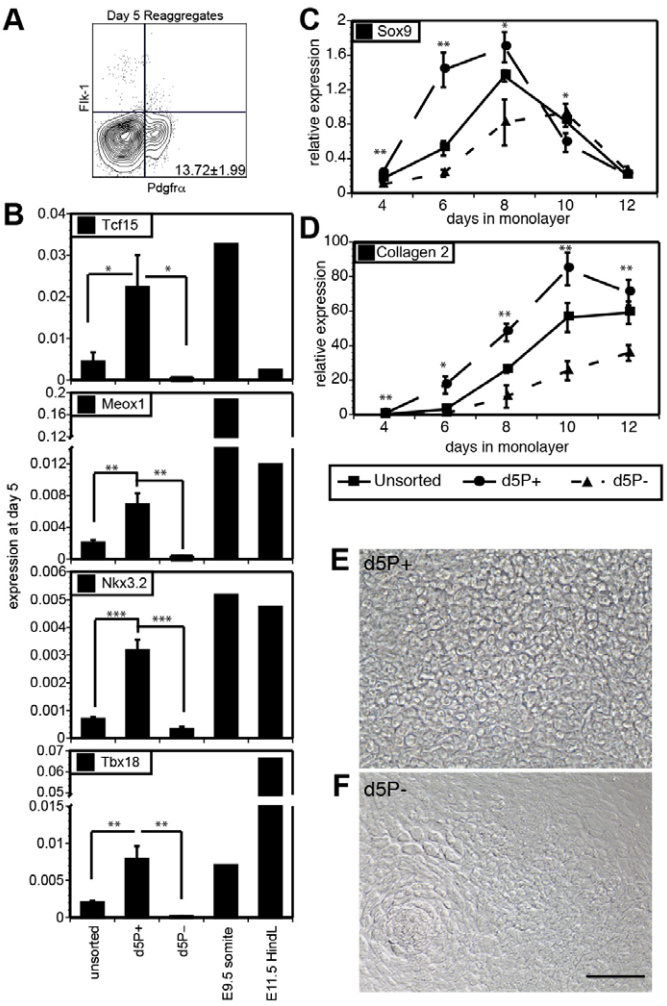

Fig. 4. Chondrogenic potential segregates to the Bry^{-}P^{+} fraction. (**A**) FACS analysis of noggin-induced aggregates on day 5. (**B-D**) Q-PCR analysis of (B) *Tcf15*, *Meox1*, *Nkx3.2*, *Tbx18*, (C) *Sox9* and (D) collagen 2 expression in unsorted populations and in the Bry^{-}P^{+} (d5P^{+}) and Bry^{-}P^{-} (d5P^{-}) populations isolated from day 5 aggregates as indicated. Significance in d5P^{+}-derived monolayers was compared with d5P^{-} cultures. E9.5 somites and E11.5 hindlimbs (HindL) were used as controls. (**E**,**F**) Morphology of monolayers derived from (E) d5P^{+} or (F) d5P^{-} populations following 11 days of culture. Scale bar: 100 μm. Error bars indicate s.e.m. (n=3-6). *P<0.05, **P<0.01, ***P<0.001.

fibroblastic-like cells. Gene expression analyses during monolayer differentiation demonstrated interesting similarities as well as differences (Fig. 5C-L). Both populations showed similar levels and temporal patterns of *Sox9* expression (Fig. 5C), which peaked at day 8 and declined sharply by day 12. Increased levels of collagen 2 expression was observed after the peak of *Sox9* expression in both populations, although the levels were somewhat higher in the BMP4-treated cells (Fig. 5D). Expression of *Sox9* and collagen 2 confirms that chondrogenesis had occurred in both cultures.

Genes associated with GPCs, hypertrophy and angiogenesis/vascularization [collagen 10 (Col10a1), collagen 1, *Vegf* (*Vegfa*), osterix (*Sp7* – Mouse Genome Informatics)] were expressed at significantly higher levels in end-stage BMP4-treated cultures compared with Gdf5-treated cells (Fig. 5E-H). By contrast, lubricin (*Prg4* – Mouse Genome Informatics), a gene expressed in ACs, was detected at significantly higher levels in Gdf5-treated cells (Fig. 5I). Genes associated with joint interzone development or function, including *Wnt9a* (Archer et al., 2003; Pacifici et al., 2006) and doublecortin (Zhang et al., 2011; Zhang et al., 2007), as well as the BMP inhibitor sclerostin domain-containing protein 1 (*Sostdc1*) (Guo et al., 2010; Knosp et al., 2007), were also found to be expressed at significantly higher levels in Gdf5-treated cells than in the BMP4-treated populations (Fig. 5J-L). The presence of chondrocytes in both cultures, and the observed differential expression patterns, support the interpretation that the BMP4-treated population represents hypertrophic growth plate-like chondrocytes whereas the Gdf5-treated population contains non-hypertrophic articular-like chondrocytes potentially derived from an interzone-like intermediate population.

Formation of tissue *in vitro*

To evaluate further the potential of the BMP4- and Gdf5-treated populations, cells from each were seeded onto membrane filters to generate three-dimensional tissues with ECM that can be visualized histologically after several weeks (Fig. 6A). Within 2 weeks, both populations generated cartilaginous tissue that showed metachromatic staining with Toluidine Blue and expressed collagen 2 and focal collagen 10 protein (Fig. 6B). Gdf5-treated chondrocytes consistently gave rise to cartilaginous tissue that appeared thicker and stained darker with Toluidine Blue than the tissue from BMP4-treated cells, indicating higher levels of proteoglycans. The presence of collagen 10 in the tissue derived from the Gdf5-treated cells was somewhat unexpected, as the day 12 monolayers from which the tissue was generated did not express significant levels of this gene.

In an attempt to reduce the hypertrophy and collagen 10 expression in the Gdf5-treated population, we manipulated additional signaling pathways during the monolayer stage. As a first step, we investigated the role of the Hedgehog (Hh) pathway as it is involved in GPC maturation (Long et al., 2001; Minina et al., 2001) and inhibition of the pathway promotes an AC phenotype in limb explant cells (Lin et al., 2009). Addition of the Hh inhibitor cyclopamine (cyc) (Chen et al., 2002; Taipale et al., 2000) in combination with Gdf5 (Gdf+cyc) during monolayer culture did not significantly impact gene expression patterns, with the exception of those immediately responsive to Hh signaling (supplementary material Fig. S5). Tissue derived from Gdf5+cyc-treated cells was spatially organized with columnar chondrocytes at the basal layer, a collagen 2-rich tidemark, and a distinct superficial layer (Fig. 6B). Collagen 10 was still detected in the Gdf5+cyc-derived tissue, and was localized to chondrocytes exhibiting a hypertrophic phenotype at the basal surface of the tissue.

Interzone cells and ACs express the BMP inhibitors chordin and noggin, and the BMP-binding ECM molecule asporin (Brunet et al., 1998; Tardif et al., 2006; Yasuhara et al., 2011), suggesting that the level of BMP activation might influence the development and/or maintenance of this population. Bmp4 binds to both Bmpr1α and Bmpr1β type I receptors, whereas Gdf5 signals primarily through Bmpr1β. Given these differences, we were able to specifically inhibit endogenous Bmp4 signaling during Gdf5 treatment by the addition of soluble Bmpr1α (sBmpr1α). sBmpr1α did not significantly affect gene expression patterns in the day 12 monolayers (supplementary material Fig. S5). Tissues derived from cells treated with Gdf5, Gdf5+cyc, Gdf5+sBmpr1α, and Gdf5+sBmpr1α+cyc (hereafter referred to as G1αC) were analyzed after 5 weeks (Fig. 6C). Collagen 10 expression was detected in the tissue generated from Gdf5-, Gdf5+cyc- and Gdf5+sBmpr1α-treated cells (Fig. 6C), indicating that sBmpr1α alone was not sufficient to prevent collagen 10 expression. However, treatment

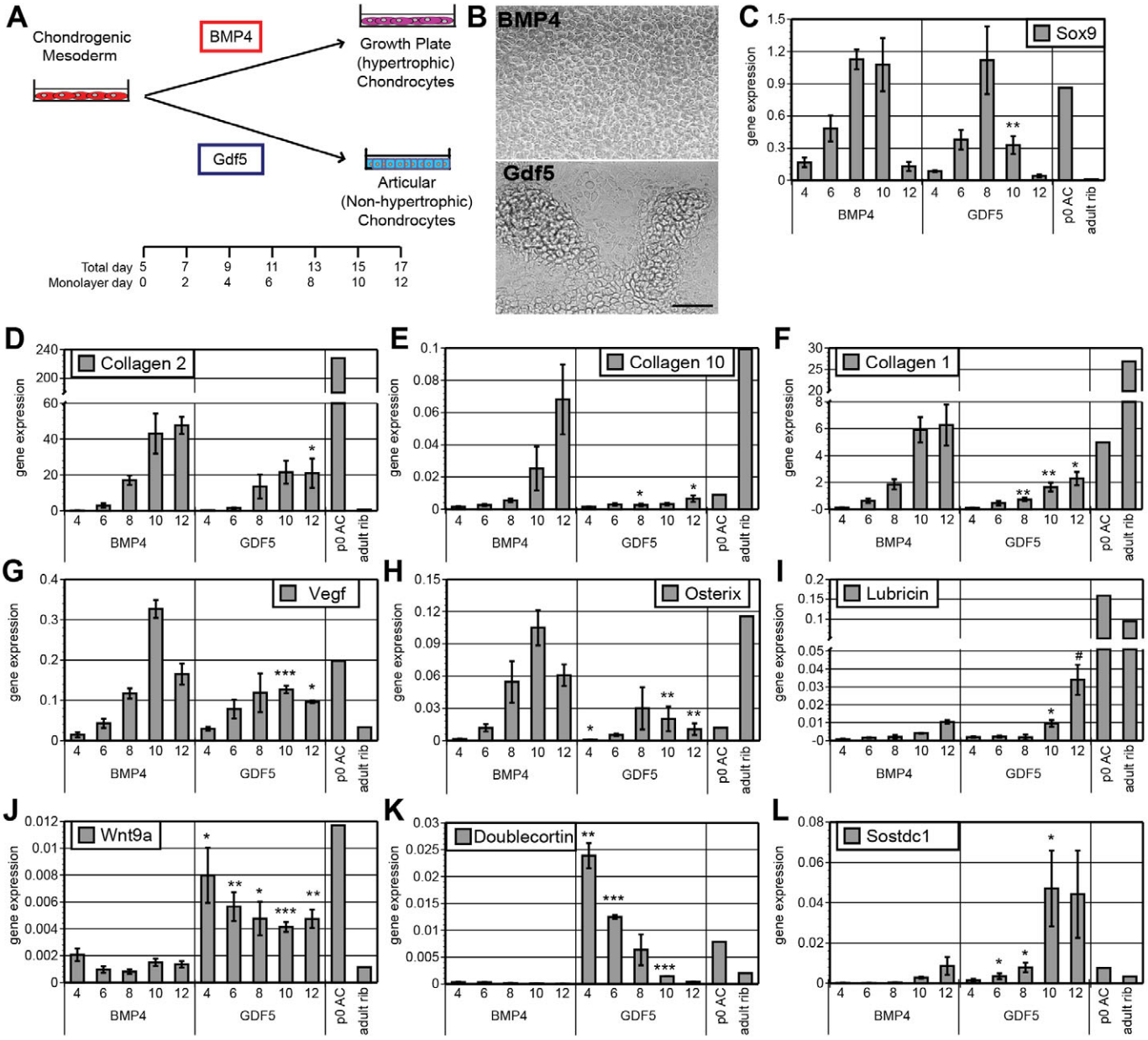

Fig. 5. Generation of hypertrophic and non-hypertrophic chondrocytes from mESC-derived chondrogenic mesoderm. (**A**,**B**) Protocol for monolayer culture for 4-12 days (A) and representative micrographs of chondrocytes (B) treated with BMP4 or Gdf5. Scale bar: 100 μm. (**C-L**) Q-PCR analysis of (C) *Sox9*, (D) collagen 2, (E) collagen 10, (F) collagen 1, (G) *Vegf*, (H) osterix, (I) lubricin, (J) *Wnt9a*, (K) doublecortin and (L) *Sostdc1* expression during monolayer culture at the indicated times. Primary ACs and adult rib cartilage were used as controls. Error bars indicate s.e.m. (n=3). *P<0.05, **P<0.01, ***P<0.001, $^{\#}P$=0.0546. Significance of each Gdf5-treated time point was compared with corresponding BMP4 time point.

with both inhibitors (G1αC) consistently resulted in cartilage-like tissue that expressed high levels of collagen 2 (supplementary material Fig. S6), but virtually no collagen 10, suggesting that tissue containing non-hypertrophic chondrocytes was generated *in vitro*. By contrast, the BMP4-derived and other Gdf5-derived tissues expressed both collagen 2 and collagen 10, and as such represent cartilage tissue comprising hypertrophic chondrocytes. These observations indicate that through manipulation of the Hh, BMP and Gdf5 pathways, it is possible to specify two unique chondrocyte populations that generate tissues *in vitro* that display characteristics of articular (G1αC-treatment) and growth plate (BMP4-treatment) cartilage.

Potential of hypertrophic and non-hypertrophic mESC-derived chondrocytes *in vivo*

Given the potential of the mESC-derived chondrocytes to form tissue *in vitro*, we next sought to determine their ability to generate cartilage *in vivo*. To enable us to distinguish mESC-derived cells from host cells, we used a GFP-Bry mESC line that constitutively expresses the red fluorescent protein (RFP) (Luche et al., 2007). $Bry^{-}P^{+}RFP^{+}$ cells isolated by fluorescence-activated cell sorting (FACS) from day 5 aggregates were cultured in the presence of either BMP4 or G1aC for 12 days. Following monolayer culture, cells were injected subcutaneously into immunodeficient mice. Developing tissue was easily identified after 2, 4 and 8 weeks as

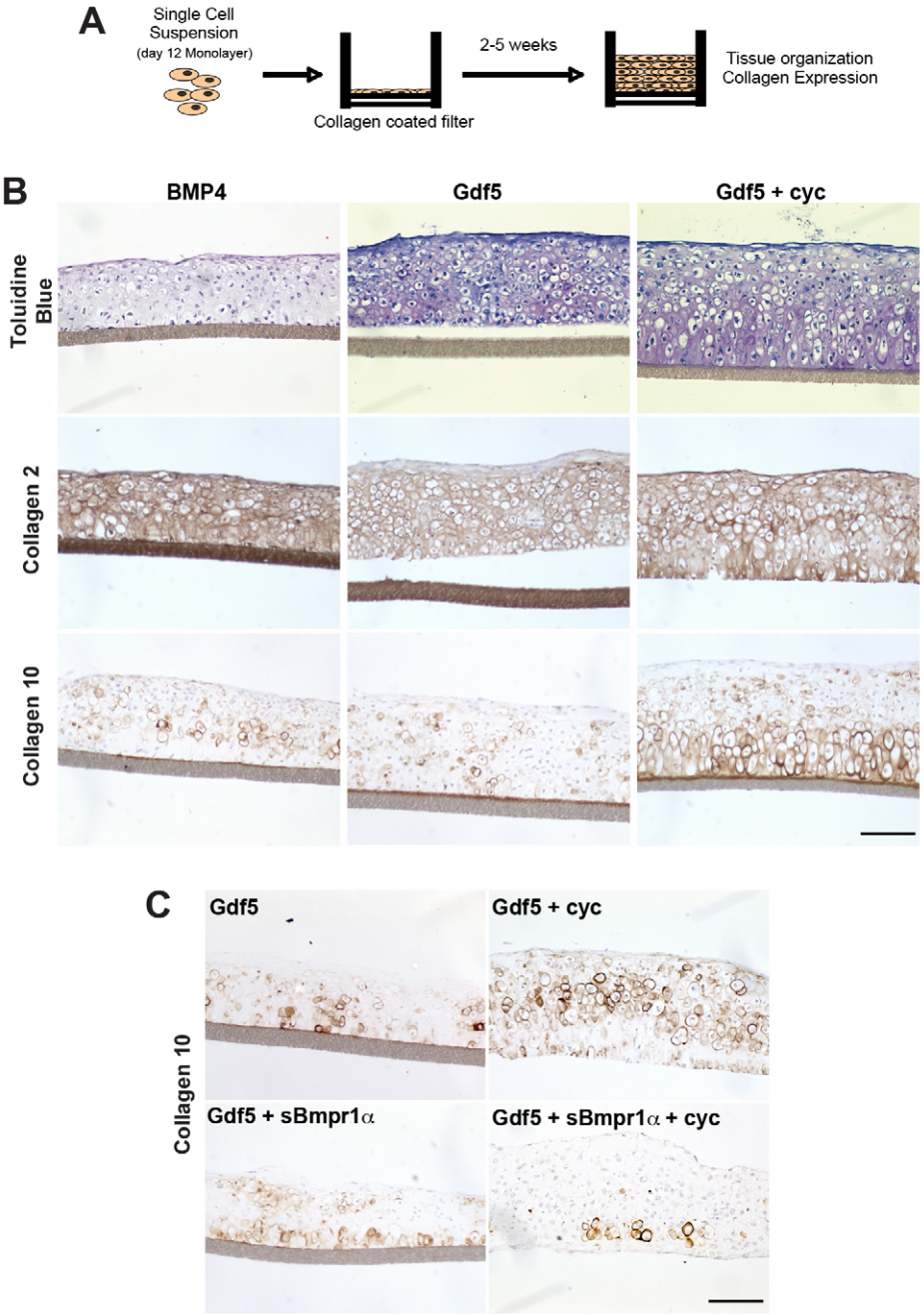

Fig. 6. mESC-derived chondrocytes generate three-dimensional cartilage-like tissue *in vitro*. (**A**) Chondrocytes derived in the presence of the indicated factors were cultured on collagen 2-coated filters for 2-5 weeks. (**B**,**C**) Tissues following 2 (B) and 5 (C) weeks of culture stained with Toluidine Blue, or with antibodies against collagen 2 and collagen 10 as indicated. Scale bars: 100 μm.

white or clear structures under the skin. All grafts were vascularized by 4-8 weeks (not shown). Von Kossa staining revealed the presence of mineralized cartilage or bone in 8-week-old grafts derived from both the BMP4- and G1αC-induced chondrocytes (Fig. 7A), suggesting that both had undergone endochondral ossification. At an earlier time point, areas of cartilage tissue were identified (Safranin O positivity) in the grafts derived from both cell types (Fig. 7B,C), and hypertrophic chondrocytes were observed in most grafts by 4 weeks (Fig. 7B,C, arrows). Whereas mESC-derived cells (RFP^+) were detected at all time points, host-derived cells (RFP^-) were identified after 4 weeks, suggesting that host cells were recruited to the site of engraftment. Although these data demonstrate that both populations of mESC-derived chondrocytes have the capacity to generate cartilage-like tissue following transplantation *in vivo*, the presence of bone in most grafts indicates that either hypertrophic chondrocytes are present in both populations, or the site of transplantation might not be suitable for the maintenance of stable cartilage *in vivo*.

To address the suitability of the site of transplantation for maintenance of stable cartilage, two additional transplantation models were explored. As articular cartilage is avascular, we next transplanted the mESC-derived cartilage tissue in a diffusion chamber into recipient mice to prevent host vascularization. Four weeks following transplantation, no bone-like tissue was observed within the cartilage-like tissue contained in the diffusion chamber (supplementary material Fig. S7A). The tissue generated by G1αC-induced cells was thicker than tissue derived from BMP4-induced chondrocytes. Although these differences were observed, chondrocytes in both tissues did exhibit a hypertrophic morphology, indicating that the environment within the chamber did not support the maintenance of the non-hypertrophic chondrocytes. In contrast to tissues in the chamber, tissues transplanted subcutaneously

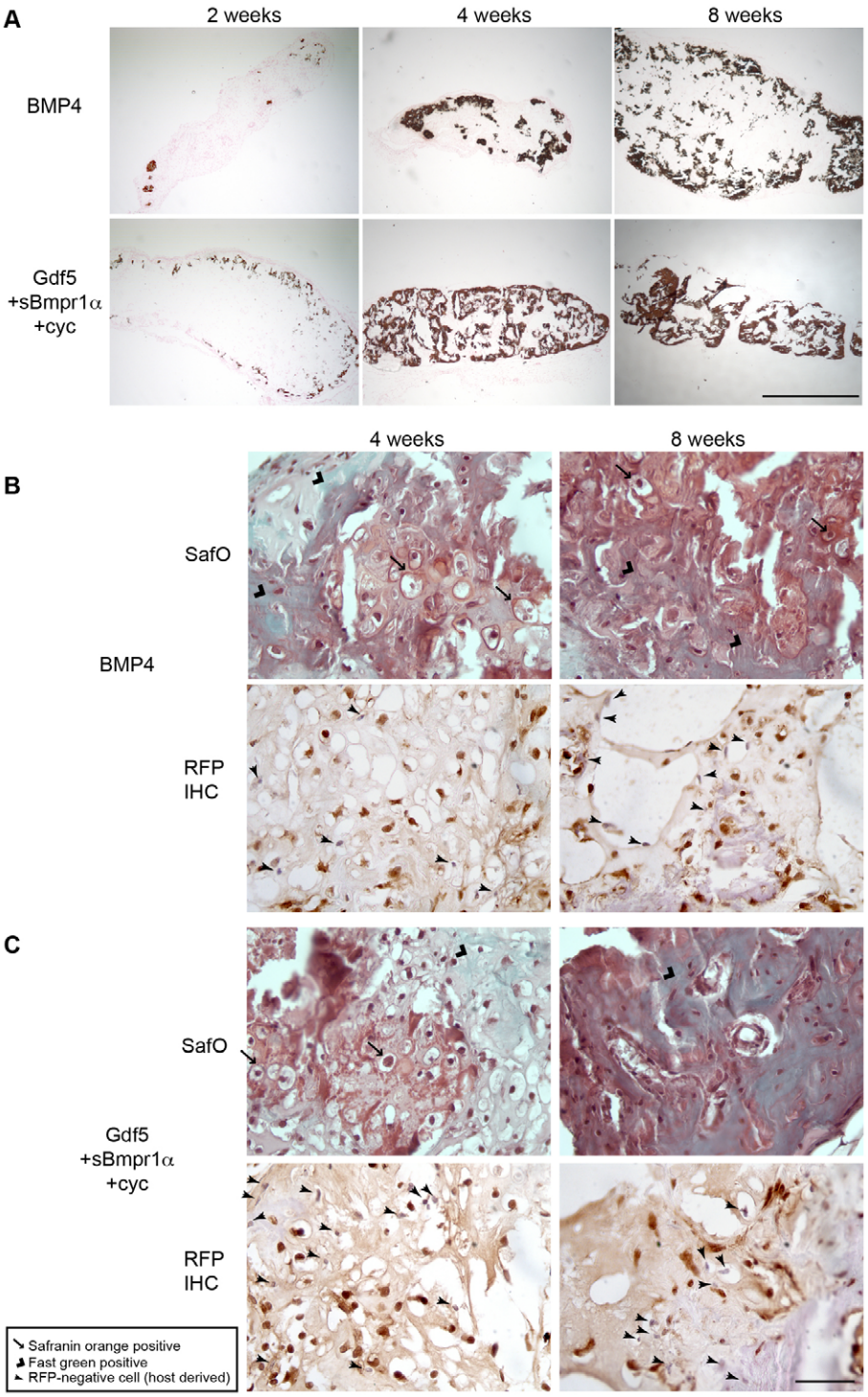

Fig. 7. mESC-derived chondrocytes generate cartilage-like tissue that undergoes ossification *in vivo*. (**A-C**) BMP4- or G1αC-treated RFP.bry mESCs were injected subcutaneously at the mammary fat pad site. Grafts were harvested up to 8 weeks post-injection as indicated, processed for histology and stained with von Kossa (A) or Safranin O (SafO; B,C, arrows) with Fast Green counterstain (chevrons). Immunohistochemistry for RFP indicates mESC-derived cells (B,C). Few host-derived cells (RFP-negative) were detected within grafts (arrowheads). Scale bars: 1 mm in A; 50 μm in B,C.

without the chamber were completely ossified within this time (supplementary material Fig. S7B), suggesting that the site of transplantation and/or the local environment or niche influences the differentiation potential of the grafted cells. Although cartilage tissue was clearly present in the diffusion chambers after 4 weeks, chondrocyte survival was compromised, possibly owing to apoptosis associated with hypertrophic differentiation or to poor diffusion across the chamber.

mESC-derived chondrocyte populations were also transplanted into transgenic mice that contain the herpes simplex virus thymidine kinase (TK) gene under control of an osteoblast-specific collagen 1 promoter (DTK^+ mice). With this model, host osteoblasts are depleted following administration of gancyclovir. When transplanted into DTK^+ mice, both BMP4-treated and G1αC-treated chondrocytes generated cartilage-like engraftments containing little to no bone-like tissue after 8 weeks. By contrast, grafts in control DTK^- mice contained, on average, >20% bone-like tissue (Table 1; Fig. 8). These observations indicate that, in the absence of host osteoblasts, mESC-derived cartilage-like tissue does not undergo extensive ossification.

Table 1. Scores of engraftments containing bone-like tissue in the DTK transgenic mouse model

Cells	Total engraftments	Average score	Score ≤1.5	Score ≥1.5
BMP4-induced cells				
DTK$^-$	8	2.21	2	6
DTK$^+$	6	1.55	4	2
G1αC-induced cells				
DTK$^-$	6	2.74	0	6
DTK$^+$	15	1.58	9	6

Scores represent the percentage of bone-like tissue contained within engraftment: 1, <5% bone-like tissue; 2, 5-20% bone-like tissue; 3, >20% bone-like tissue. Scores represent an average of three scores assessed for each engraftment over a broad range of sections (i.e. slides 10, 20 and 30) stained with Safranin O/Fast Green with adjacent sections with H&E. Three independent blind scores were obtained per section.

DISCUSSION

Previous studies have demonstrated that it is possible to generate chondrocytes from ESCs and, through the stage-specific manipulation of different signaling pathways, have established parameters for the generation of chondrogenic mesoderm *in vitro*. By further translating our understanding of chondrocyte development in the embryo to the differentiation cultures, we have been able to build on these findings and, in this study, provide the following new insights into mESC-derived chondrocyte development and tissue formation *in vitro* and *in vivo*. First, we have defined the temporal emergence of chondrogenic mesoderm in mESC differentiation cultures and demonstrate that it develops as an F$^-$P$^+$ population following the appearance of an early F$^-$P$^+$ cardiogenic mesoderm population. Second, we provide evidence that treatment of the ESC-derived chondrogenic mesoderm with different pathway agonists promotes the development of distinct populations that display differences in cellular hypertrophy as well as in other characteristics of GPCs and ACs. Our interpretation of these differences is that the BMP4-induced hypertrophic cells represent GPCs, whereas the Gdf5-induced population represents ACs. Third, we have shown that these chondrocyte populations are able to generate highly organized tissue *in vitro* that displays some features of GPC and articular cartilage tissues, respectively. Formal demonstration that the *in vitro*-generated tissues do indeed represent different types of cartilage will require further transplantation experiments, under conditions in which one undergoes ossification, whereas the other persists as cartilage with articular characteristics. Finally, we demonstrate that ESC-derived chondrocytes and cartilage-like tissues are able to undergo an ossification process *in vivo* resembling the process that occurs during embryonic development and in the adolescent animal. However, in the absence of host osteoblasts or vascularization, these chondrocytes are able to generate and maintain cartilage tissue *in vivo* with little to no bone formation.

We have shown that induction of F$^-$P$^+$ chondrogenic mesoderm does not require BMP signaling, whereas F$^+$P$^+$ mesoderm that gives rise to the hematopoietic and cardiac lineages is dependent on this pathway. This confirms previous results from our laboratory (Kattman et al., 2011; Nostro et al., 2008) and those of Tanaka et al. (Tanaka et al., 2009), and highlights important differences in the signaling requirements for the generation of mesodermal populations that can be exploited for enrichment purposes. Although our previous studies have defined cardiovascular mesoderm as an F$^+$P$^+$ population (Kattman et al., 2011), our findings here demonstrate that the noggin-induced F$^-$P$^+$ population also displays some cardiogenic potential. These differences might simply reflect the fact that the F$^-$P$^+$ population is less mature than the F$^+$P$^+$ population, and that the cells will upregulate Flk-1 as they mature. Alternatively, F$^-$P$^+$ cells might give rise to cardiomyocytes that

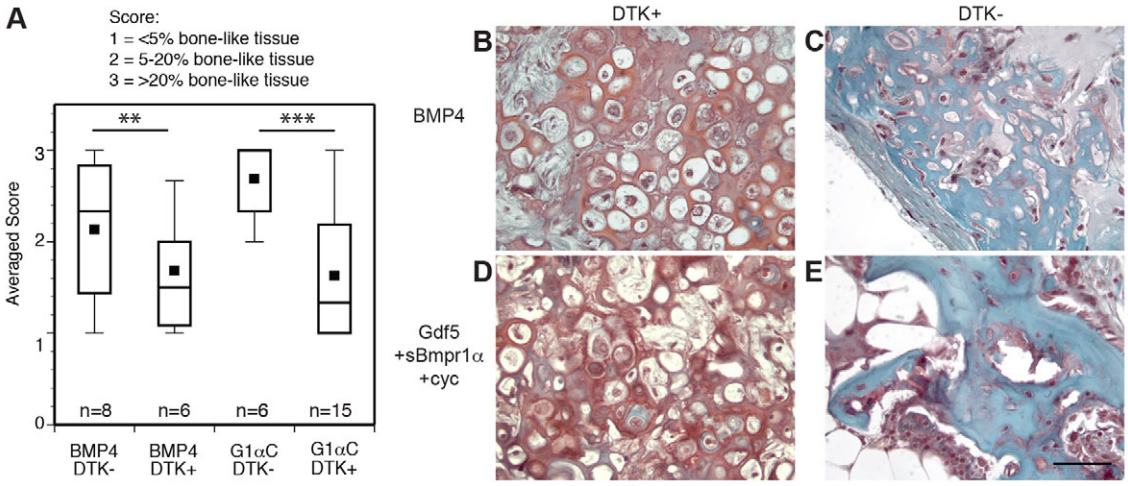

Fig. 8. mESC-derived chondrocytes generate cartilage-like tissue in the absence of osteoblasts. (**A**) Scores of engrafted tissues generated from BMP4- or Gdf5+sBmpr1α+cyc-treated cells in DTK$^+$ and DTK$^-$ mice. Scores represent the percentage of bone-like tissue contained within the graft as an average of three scores assessed for each engraftment over a broad range of sections (i.e. slides 10, 20 and 30) stained with Safranin O/Fast Green with adjacent sections stained with H&E. Student's *t*-test was used to evaluate statistical significance. Boxes indicate first and third quartiles of data set; whiskers indicate minimum and maximum of all the data; horizontal line indicates median; square indicates mean (average score). (**B-E**) Representative 8-week grafts stained with Safranin O: BMP4-treated cells in DTK$^+$ mouse (B, score 1) and DTK$^-$ mouse (C, score 3); G1αC-treated cells in DTK$^+$ mouse (D, score 1) and DTK$^-$ mouse (E, score 3). Scale bar: 50 μm.

differ from those generated by F^+P^+ cells. Current studies are aimed at investigating this possibility. The emergence of the F^-P^+ cardiac mesoderm before the F^-P^+ chondrogenic mesoderm accurately recapitulates the temporal allocation of these mesoderm fates in the early embryo, once again demonstrating that lineage development in this *in vitro* model system faithfully mimics lineage development in the embryo (Kinder et al., 1999; Lawson et al., 1991). By taking advantage of these temporal differences, it was possible to develop strategies to generate populations of highly enriched chondrocytes.

Access to a highly enriched population of chondrogenic mesoderm enabled us to investigate the signaling pathways that regulate the specification of chondrocytes that display either hypertrophic growth plate-like or non-hypertrophic articular-like characteristics. Consistent with the findings of others using ESCs and our understanding of the regulation of the lineage *in vivo* (Hatakeyama et al., 2004; Tsumaki et al., 2002; Yoon et al., 2006), we found that BMP4 signaling did promote the development of chondrocytes that display gene expression patterns indicative of hypertrophic growth plate-like chondrocytes. When stimulated with Gdf5, however, cells with gene expression profiles consistent with interzone cells and ACs emerged. Lineage-tracing studies and detailed expression analyses have shown that Gdf5 is expressed in the emerging ACs as well as in the cells surrounding this population (Koyama et al., 2008; Rountree et al., 2004). These observations are consistent with a role of this factor in inducing and/or promoting the expansion of these chondrocytes. Although the ability to generate chondrocyte populations with different characteristics by specification with different factors supports the interpretation that they derive from distinct progenitors, the role of the environment in maintaining distinct phenotypes was clearly demonstrated by the *in vivo* studies presented in this report.

Bmp4 and Gdf5, both members of the TGFβ superfamily, have different functions during the formation of synovial joints, cartilage and bone and, in this study, specify distinct subsets of mESC-derived chondrocytes that display different characteristics. A comparison of Bmp4 and Gdf5 in embryonic limb micromasses demonstrated that Bmp4 treatment induced chondrogenesis and collagen 2 expression in all cells (within cartilage-like nodules and in internodular spaces), whereas an increase in the number of cartilage nodules was observed after Gdf5 treatment (Hatakeyama et al., 2004). These effects are somewhat recapitulated in the mESC-derived monolayer cultures as BMP4 induced a homogeneous chondrocytes population, whereas Gdf5 treatment induced populations of condensed nodules together with fibroblastic cells. The effects of both BMP4 and Gdf5 appear to be mediated through Bmpr1-dependent phosphorylation events as concurrent treatment with dorsomorphin (Yu et al., 2008) at high concentrations impaired cell survival and at lower concentrations prevented the upregulation of chondrogenic genes (supplementary material Fig. S8A-C).

When cultured on membrane filters, ESC-derived chondrocyte populations generated cartilage-like tissue that was rich in collagens and proteoglycans and highly organized into zones of cartilage normally found in articular joints. These findings are the first documentation of tissue formation from ESC-derived chondrocytes without the requirement of co-culture or seeding onto a scaffold. Although our molecular analyses showed low levels of expression of the hypertrophic marker collagen 10 in the Gdf5-induced chondrocyte population, cartilage-like tissue generated from it clearly contained collagen 10-expressing hypertrophic cells. By contrast, populations specified in the presence of Gdf5 together with hedgehog- and Bmp4-specific inhibitors (G1αC treatment) generated tissue that showed markedly reduced numbers of collagen 10-expressing hypertrophic chondrocytes. These findings suggest that low levels of endogenous Bmp4 and hedgehog signaling maintain some hypertrophic chondrocytes in the Gdf5-treated cultures and inhibition of these pathways during the chondrocyte specification step reduces the number of these contaminating cells. These observations are consistent with the known role of these pathways in chondrocyte development *in vivo*. There is no detectable hedgehog signaling in the region of AC development whereas it is active in the growth plate (Long et al., 2001). Bmp4 is also not expressed in mature ACs, which express chordin, a potent inhibitor of the pathway (Tardif et al., 2006). Given that Bmp4 signaling is required for chondrocyte hypertrophy (Yoon et al., 2006) and is inhibited in non-hypertrophic chondrocytes under normal conditions, it is possible that activation of the pathway in non-hypertrophic chondrocyte populations might initiate a hypertrophic response. Access to tissue with characteristics of ACs will provide a unique opportunity to identify and characterize factors and signaling pathways that induce hypertrophy and possibly play a role in the initiation of OA pathogenesis.

Our analysis indicated that, whereas non-hypertrophic and hypertrophic chondrocyte-enriched populations and respective cartilage-like tissues had been generated *in vitro*, grafts were ossified when subcutaneously transplanted *in vivo*. Although bone formation was anticipated from the hypertrophic chondrocyte-derived grafts, it was unexpected from the grafts generated with non-hypertrophic chondrocytes and tissues. It is possible that low numbers of hypertrophic chondrocytes still contaminate the G1αC cultures and derivative tissues, which initiate ossification over time *in vivo*. Further enrichment of these populations will depend on the identification of lineage-specific markers and corresponding antibodies to allow isolation of non-hypertrophic (AC-like) and hypertrophic (GPC-like) chondrocytes by flow-cytometric approaches. Alternatively, these observations might indicate that the microenvironment of the graft was incompatible with maintenance of stable cartilage. It is possible that BMPs or other factors expressed at the graft site might initiate a conversion of non-hypertrophic chondrocytes to become hypertrophic and display additional characteristics of GPCs. Transplantation into the correct 'niche' in the joint space together with mechanical loading might be essential to maintain articular cartilage *in vivo*. Indeed, mESC-derived cartilage isolated from the host vasculature system by diffusion chamber or cartilage tissues generated in the absence of host osteoblasts were not ossified. These observations support the hypothesis that the correct niche would be required to support the maintenance of non-hypertrophic articular-like cartilage derived from PSCs.

In summary, the findings presented here have established the developmental program for chondrogenic mesoderm formation from mESCs and have identified regulatory pathways that play a role in the specification of this mesoderm to both hypertrophic and non-hypertrophic chondrocytes. These advances enable us for the first time to generate cartilage-like tissue that has the characteristics of articular and growth plate cartilage *in vitro*, providing a model for further investigating pathways that regulate these fates and/or maintain this stable cartilage tissue under normal conditions, as well as for identifying factors that may initiate changes indicative of the early stages of disease such as OA. Access to highly enriched populations of non-hypertrophic articular-like chondrocytes and to cartilage tissue derived from them provides the first opportunity to begin to test the feasibility of developing cell and tissue replacement therapy for the treatment of OA. The translation of these findings to human PSCs will be instrumental for the development of such applications for the treatment of human disease.

Acknowledgements
We thank the Flow Cytometry Facility at the Hospital for Sick Children for cell sorting; Richard Renlund, Frank Guiliani and Sarah Wilson at the University of Toronto Division of Comparative Medicine for assistance in animal studies; Mona Reid, Clara Goodwin and Heather Whetstone for histological services; and members of the G.M.K. laboratory for critical reading of the manuscript.

Funding
This work was supported by a grant from the Canadian Institutes of Health Research (CIHR) [MOP 219710] to B.A.A. and G.M.K.

Competing interests statement
The authors declare no competing financial interests.

Supplementary material
Supplementary material available online at
http://dev.biologists.org/lookup/suppl/doi:10.1242/dev.087890/-/DC1

References

Ahmed, N., Gan, L., Nagy, A., Zheng, J., Wang, C. and Kandel, R. A. (2009). Cartilage tissue formation using redifferentiated passaged chondrocytes in vitro. *Tissue Eng. Part A* **15**, 665-673.
Akiyama, H., Chaboissier, M. C., Martin, J. F., Schedl, A. and de Crombrugghe, B. (2002). The transcription factor Sox9 has essential roles in successive steps of the chondrocyte differentiation pathway and is required for expression of Sox5 and Sox6. *Genes Dev.* **16**, 2813-2828.
Archer, C. W., Dowthwaite, G. P. and Francis-West, P. (2003). Development of synovial joints. *Birth Defects* **69**, 144-155.
Blumer, M. J., Longato, S., Schwarzer, C. and Fritsch, H. (2007). Bone development in the femoral epiphysis of mice: the role of cartilage canals and the fate of resting chondrocytes. *Dev. Dyn.* **236**, 2077-2088.
Brunet, L. J., McMahon, J. A., McMahon, A. P. and Harland, R. M. (1998). Noggin, cartilage morphogenesis, and joint formation in the mammalian skeleton. *Science* **280**, 1455-1457.
Burgess, R., Rawls, A., Brown, D., Bradley, A. and Olson, E. N. (1996). Requirement of the paraxis gene for somite formation and musculoskeletal patterning. *Nature* **384**, 570-573.
Bussen, M., Petry, M., Schuster-Gossler, K., Leitges, M., Gossler, A. and Kispert, A. (2004). The T-box transcription factor Tbx18 maintains the separation of anterior and posterior somite compartments. *Genes Dev.* **18**, 1209-1221.
Chen, J. K., Taipale, J., Cooper, M. K. and Beachy, P. A. (2002). Inhibition of Hedgehog signaling by direct binding of cyclopamine to Smoothened. *Genes Dev.* **16**, 2743-2748.
Colnot, C. (2005). Cellular and molecular interactions regulating skeletogenesis. *J. Cell. Biochem.* **95**, 688-697.
Dacquin, R., Starbuck, M., Schinke, T. and Karsenty, G. (2002). Mouse alpha1(I)-collagen promoter is the best known promoter to drive efficient Cre recombinase expression in osteoblast. *Dev. Dyn.* **224**, 245-251.
Dao, D. Y., Jonason, J. H., Zhang, Y., Hsu, W., Chen, D., Hilton, M. J. and O'Keefe, R. J. (2012). Cartilage-specific β-catenin signaling regulates chondrocyte maturation, generation of ossification centers, and perichondrial bone formation during skeletal development. *J. Bone Miner. Res.* **27**, 1680-1694.
Darabi, R., Gehlbach, K., Bachoo, R. M., Kamath, S., Osawa, M., Kamm, K. E., Kyba, M. and Perlingeiro, R. C. (2008). Functional skeletal muscle regeneration from differentiating embryonic stem cells. *Nat. Med.* **14**, 134-143.
Fehling, H. J., Lacaud, G., Kubo, A., Kennedy, M., Robertson, S., Keller, G. and Kouskoff, V. (2003). Tracking mesoderm induction and its specification to the hemangioblast during embryonic stem cell differentiation. *Development* **130**, 4217-4227.
Fletcher, R. B. and Harland, R. M. (2008). The role of FGF signaling in the establishment and maintenance of mesodermal gene expression in Xenopus. *Dev. Dyn.* **237**, 1243-1254.
Gadue, P., Huber, T. L., Paddison, P. J. and Keller, G. M. (2006). Wnt and TGF-beta signaling are required for the induction of an in vitro model of primitive streak formation using embryonic stem cells. *Proc. Natl. Acad. Sci. USA* **103**, 16806-16811.
Gouon-Evans, V., Boussemart, L., Gadue, P., Nierhoff, D., Koehler, C. I., Kubo, A., Shafritz, D. A. and Keller, G. (2006). BMP-4 is required for hepatic specification of mouse embryonic stem cell-derived definitive endoderm. *Nat. Biotechnol.* **24**, 1402-1411.
Guo, S., Zhou, J., Gao, B., Hu, J., Wang, H., Meng, J., Zhao, X., Ma, G., Lin, C., Xiao, Y. et al. (2010). Missense mutations in IHH impair Indian Hedgehog signaling in C3H10T1/2 cells: implications for brachydactyly type A1, and new targets for Hedgehog signaling. *Cell. Mol. Biol. Lett.* **15**, 153-176.
Hatakeyama, Y., Tuan, R. S. and Shum, L. (2004). Distinct functions of BMP4 and GDF5 in the regulation of chondrogenesis. *J. Cell. Biochem.* **91**, 1204-1217.
Hirsinger, E., Jouve, C., Dubrulle, J. and Pourquié, O. (2000). Somite formation and patterning. *Int. Rev. Cytol.* **198**, 1-65.
Hwang, N. S., Kim, M. S., Sampattavanich, S., Baek, J. H., Zhang, Z. and Elisseeff, J. (2006). Effects of three-dimensional culture and growth factors on the chondrogenic differentiation of murine embryonic stem cells. *Stem Cells* **24**, 284-291.
Hwang, Y. S., Polak, J. M. and Mantalaris, A. (2008). In vitro direct chondrogenesis of murine embryonic stem cells by bypassing embryoid body formation. *Stem Cells Dev.* **17**, 971-978.
Jukes, J. M., Both, S. K., Leusink, A., Sterk, L. M., van Blitterswijk, C. A. and de Boer, J. (2008). Endochondral bone tissue engineering using embryonic stem cells. *Proc. Natl. Acad. Sci. USA* **105**, 6840-6845.
Kattman, S. J., Witty, A. D., Gagliardi, M., Dubois, N. C., Niapour, M., Hotta, A., Ellis, J. and Keller, G. (2011). Stage-specific optimization of activin/nodal and BMP signaling promotes cardiac differentiation of mouse and human pluripotent stem cell lines. *Cell Stem Cell* **8**, 228-240.
Kinder, S. J., Tsang, T. E., Quinlan, G. A., Hadjantonakis, A. K., Nagy, A. and Tam, P. P. (1999). The orderly allocation of mesodermal cells to the extraembryonic structures and the anteroposterior axis during gastrulation of the mouse embryo. *Development* **126**, 4691-4701.
Knosp, W. M., Saneyoshi, C., Shou, S., Bächinger, H. P. and Stadler, H. S. (2007). Elucidation, quantitative refinement, and in vivo utilization of the HOXA13 DNA binding site. *J. Biol. Chem.* **282**, 6843-6853.
Koyama, E., Shibukawa, Y., Nagayama, M., Sugito, H., Young, B., Yuasa, T., Okabe, T., Ochiai, T., Kamiya, N., Rountree, R. B. et al. (2008). A distinct cohort of progenitor cells participates in synovial joint and articular cartilage formation during mouse limb skeletogenesis. *Dev. Biol.* **316**, 62-73.
Kramer, J., Hegert, C., Guan, K., Wobus, A. M., Müller, P. K. and Rohwedel, J. (2000). Embryonic stem cell-derived chondrogenic differentiation in vitro: activation by BMP-2 and BMP-4. *Mech. Dev.* **92**, 193-205.
Kulesa, P. M. and Fraser, S. E. (2002). Cell dynamics during somite boundary formation revealed by time-lapse analysis. *Science* **298**, 991-995.
LaPrade, R. F., Bursch, L. S., Olson, E. J., Havlas, V. and Carlson, C. S. (2008). Histologic and immunohistochemical characteristics of failed articular cartilage resurfacing procedures for osteochondritis of the knee: a case series. *Am. J. Sports Med.* **36**, 360-368.
Lawrence, R. C., Felson, D. T., Helmick, C. G., Arnold, L. M., Choi, H., Deyo, R. A., Gabriel, S., Hirsch, R., Hochberg, M. C., Hunder, G. G. et al. (2008). Estimates of the prevalence of arthritis and other rheumatic conditions in the United States. Part II. *Arthritis Rheum.* **58**, 26-35.
Lawson, K. A., Meneses, J. J. and Pedersen, R. A. (1991). Clonal analysis of epiblast fate during germ layer formation in the mouse embryo. *Development* **113**, 891-911.
Lin, A. C., Seeto, B. L., Bartoszko, J. M., Khoury, M. A., Whetstone, H., Ho, L., Hsu, C., Ali, S. A. and Alman, B. A. (2009). Modulating hedgehog signaling can attenuate the severity of osteoarthritis. *Nat. Med.* **15**, 1421-1425.
Long, F., Zhang, X. M., Karp, S., Yang, Y. and McMahon, A. P. (2001). Genetic manipulation of hedgehog signaling in the endochondral skeleton reveals a direct role in the regulation of chondrocyte proliferation. *Development* **128**, 5099-5108.
Luche, H., Weber, O., Nageswara Rao, T., Blum, C. and Fehling, H. J. (2007). Faithful activation of an extra-bright red fluorescent protein in 'knock-in' Cre-reporter mice ideally suited for lineage tracing studies. *Eur. J. Immunol.* **37**, 43-53.
Mankoo, B. S., Skuntz, S., Harrigan, I., Grigorieva, E., Candia, A., Wright, C. V., Arnheiter, H. and Pachnis, V. (2003). The concerted action of Meox homeobox genes is required upstream of genetic pathways essential for the formation, patterning and differentiation of somites. *Development* **130**, 4655-4664.
Minina, E., Wenzel, H. M., Kreschel, C., Karp, S., Gaffield, W., McMahon, A. P. and Vortkamp, A. (2001). BMP and Ihh/PTHrP signaling interact to coordinate chondrocyte proliferation and differentiation. *Development* **128**, 4523-4534.
Murakami, S., Balmes, G., McKinney, S., Zhang, Z., Givol, D. and de Crombrugghe, B. (2004). Constitutive activation of MEK1 in chondrocytes causes Stat1-independent achondroplasia-like dwarfism and rescues the Fgfr3-deficient mouse phenotype. *Genes Dev.* **18**, 290-305.
Nakayama, N., Duryea, D., Manoukian, R., Chow, G. and Han, C. Y. (2003). Macroscopic cartilage formation with embryonic stem-cell-derived mesodermal progenitor cells. *J. Cell Sci.* **116**, 2015-2028.
Ng, A., Alman, B. and Grynpas, M. (2011). Development and validation of a mouse model of adynamic bone disease (ABD). *J. Bone Miner. Res.* **Suppl. 1.**
Nostro, M. C., Cheng, X., Keller, G. M. and Gadue, P. (2008). Wnt, activin, and BMP signaling regulate distinct stages in the developmental pathway from embryonic stem cells to blood. *Cell Stem Cell* **2**, 60-71.
Ormestad, M., Astorga, J. and Carlsson, P. (2004). Differences in the embryonic expression patterns of mouse Foxf1 and -2 match their distinct mutant phenotypes. *Dev. Dyn.* **229**, 328-333.
Pacifici, M., Koyama, E., Shibukawa, Y., Wu, C., Tamamura, Y., Enomoto-Iwamoto, M. and Iwamoto, M. (2006). Cellular and molecular mechanisms of synovial joint and articular cartilage formation. *Ann. New York Acad. Sci.* **1068**, 74-86.

Pelttari, K., Winter, A., Steck, E., Goetzke, K., Hennig, T., Ochs, B. G., Aigner, T. and Richter, W. (2006). Premature induction of hypertrophy during in vitro chondrogenesis of human mesenchymal stem cells correlates with calcification and vascular invasion after ectopic transplantation in SCID mice. *Arthritis Rheum.* **54**, 3254-3266.

Pelttari, K., Steck, E. and Richter, W. (2008). The use of mesenchymal stem cells for chondrogenesis. *Injury* **39 Suppl. 1**, S58-S65.

Rountree, R. B., Schoor, M., Chen, H., Marks, M. E., Harley, V., Mishina, Y. and Kingsley, D. M. (2004). BMP receptor signaling is required for postnatal maintenance of articular cartilage. *PLoS Biol.* **2**, e355.

Singh, M. K., Petry, M., Haenig, B., Lescher, B., Leitges, M. and Kispert, A. (2005). The T-box transcription factor Tbx15 is required for skeletal development. *Mech. Dev.* **122**, 131-144.

Stadtfeld, M., Maherali, N., Breault, D. T. and Hochedlinger, K. (2008). Defining molecular cornerstones during fibroblast to iPS cell reprogramming in mouse. *Cell Stem Cell* **2**, 230-240.

Steinert, A. F., Ghivizzani, S. C., Rethwilm, A., Tuan, R. S., Evans, C. H. and Nöth, U. (2007). Major biological obstacles for persistent cell-based regeneration of articular cartilage. *Arthritis Res. Ther.* **9**, 213.

Taipale, J., Chen, J. K., Cooper, M. K., Wang, B., Mann, R. K., Milenkovic, L., Scott, M. P. and Beachy, P. A. (2000). Effects of oncogenic mutations in Smoothened and Patched can be reversed by cyclopamine. *Nature* **406**, 1005-1009.

Takakura, N., Yoshida, H., Ogura, Y., Kataoka, H., Nishikawa, S. and Nishikawa, S. (1997). PDGFR alpha expression during mouse embryogenesis: immunolocalization analyzed by whole-mount immunohistostaining using the monoclonal anti-mouse PDGFR alpha antibody APA5. *J. Histochem. Cytochem.* **45**, 883-893.

Tam, P. P. and Tan, S. S. (1992). The somitogenetic potential of cells in the primitive streak and the tail bud of the organogenesis-stage mouse embryo. *Development* **115**, 703-715.

Tanaka, M., Jokubaitis, V., Wood, C., Wang, Y., Brouard, N., Pera, M., Hearn, M., Simmons, P. and Nakayama, N. (2009). BMP inhibition stimulates WNT-dependent generation of chondrogenic mesoderm from embryonic stem cells. *Stem Cell Res.* **3**, 126-141.

Tardif, G., Pelletier, J. P., Hum, D., Boileau, C., Duval, N. and Martel-Pelletier, J. (2006). Differential regulation of the bone morphogenic protein antagonist chordin in human normal and osteoarthritic chondrocytes. *Ann. Rheum. Dis.* **65**, 261-264.

Tins, B. J., McCall, I. W., Takahashi, T., Cassar-Pullicino, V., Roberts, S., Ashton, B. and Richardson, J. (2005). Autologous chondrocyte implantation in knee joint: MR imaging and histologic features at 1-year follow-up. *Radiology* **234**, 501-508.

Tsumaki, N., Nakase, T., Miyaji, T., Kakiuchi, M., Kimura, T., Ochi, T. and Yoshikawa, H. (2002). Bone morphogenetic protein signals are required for cartilage formation and differently regulate joint development during skeletogenesis. *J. Bone Miner. Res.* **17**, 898-906.

Visnjic, D., Kalajzic, I., Gronowicz, G., Aguila, H. L., Clark, S. H., Lichtler, A. C. and Rowe, D. W. (2001). Conditional ablation of the osteoblast lineage in Col2.3deltatk transgenic mice. *J. Bone Miner. Res.* **16**, 2222-2231.

Yamashita, A., Krawetz, R. and Rancourt, D. E. (2008). Loss of discordant cells during micro-mass differentiation of embryonic stem cells into the chondrocyte lineage. *Cell Death Differ.* **16**, 278-286.

Yasuhara, R., Ohta, Y., Yuasa, T., Kondo, N., Hoang, T., Addya, S., Fortina, P., Pacifici, M., Iwamoto, M. and Enomoto-Iwamoto, M. (2011). Roles of beta-catenin signaling in phenotypic expression and proliferation of articular cartilage superficial zone cells. *Lab. Invest.* **91**, 1739-1752.

Ying, Q. L., Nichols, J., Chambers, I. and Smith, A. (2003). BMP induction of Id proteins suppresses differentiation and sustains embryonic stem cell self-renewal in collaboration with STAT3. *Cell* **115**, 281-292.

Yoon, B. S., Pogue, R., Ovchinnikov, D. A., Yoshii, I., Mishina, Y., Behringer, R. R. and Lyons, K. M. (2006). BMPs regulate multiple aspects of growth-plate chondrogenesis through opposing actions on FGF pathways. *Development* **133**, 4667-4678.

Yu, P. B., Hong, C. C., Sachidanandan, C., Babitt, J. L., Deng, D. Y., Hoyng, S. A., Lin, H. Y., Bloch, K. D. and Peterson, R. T. (2008). Dorsomorphin inhibits BMP signals required for embryogenesis and iron metabolism. *Nat. Chem. Biol.* **4**, 33-41.

Zhang, Y., Ryan, J. A., Di Cesare, P. E., Liu, J., Walsh, C. A. and You, Z. (2007). Doublecortin is expressed in articular chondrocytes. *Biochem. Biophys. Res. Commun.* **363**, 694-700.

Zhang, Q., Cigan, A. D., Marrero, L., Lopreore, C., Liu, S., Ge, D., Savoie, F. H. and You, Z. (2011). Expression of doublecortin reveals articular chondrocyte lineage in mouse embryonic limbs. *Genesis* **49**, 75-82.

zur Nieden, N. I., Kempka, G., Rancourt, D. E. and Ahr, H. J. (2005). Induction of chondro-, osteo- and adipogenesis in embryonic stem cells by bone morphogenetic protein-2: effect of cofactors on differentiating lineages. *BMC Dev. Biol.* **5**, 1.

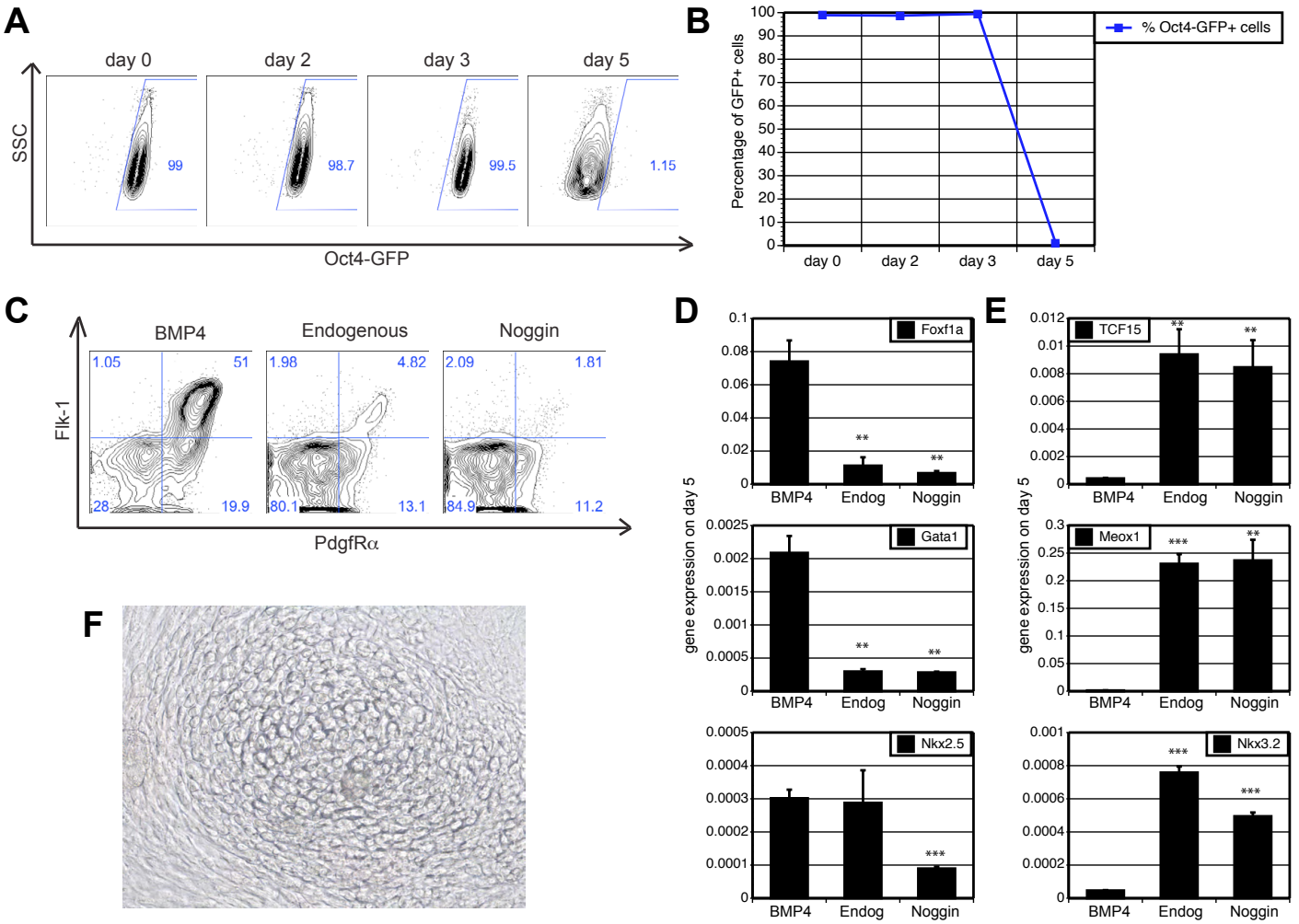

Fig. S1. BMP signaling influences mesoderm development from mouse iPSCs. Oct4-GFP miPSCs were differentiated according to the serum-free protocol shown in Fig. 1A. miPSCs were induced at day 2 for 24 hours with activin, Wnt3a, VEGF, and one of: BMP4, no BMP4 added (Endogenous, Endog), or noggin. On day 3 of culture, EBs were re-aggregated in the presence of bFGF for 2 days and then plated in monolayer culture in SFD containing BMP4 and bFGF for up to 12 days. (**A**) Flow cytometric analysis showing downregulation of Oct4-GFP over the first 5 days of differentiation (Act, Wnt3a and noggin-induced). (**B**) Quantification of GFP$^+$ cells over the course of differentiation by flow cytometry (n=6). (**C**) Flow cytometric analysis showing expression of Flk-1 and Pdgfrα after 1 day induction in indicated conditions. (**D**,**E**) Q-PCR analysis of expression of (D) the lateral plate mesoderm gene (*Foxf1a*), hematopoietic (*Gata1*) and cardiac (*Nkx2.5*) transcription factors, and (E) paraxial mesoderm (*Tcf15*) and somite (*Meox1, Nkx3.2*) genes in day 5 aggregates. Significance relative to BMP4-induced cultures. Values represent copy number relative to β-actin. *P<0.05, **P<0.01, ***P<0.001. (**F**) Micrograph of chondrocytes in monolayer culture derived from Activin, Wnt3a and noggin-induced miPSCs. Magnification 20×.

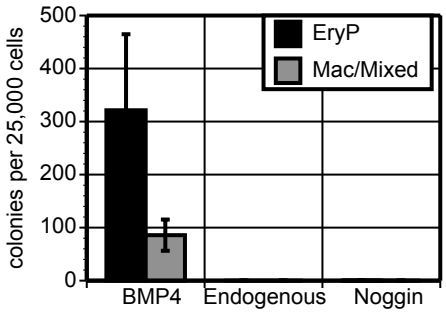

Fig. S2. Hematopoietic potential is restricted to mESC-derived cells induced with BMP4 (in combination with activin, Wnt and VEGF). Total number of primitive erythroid colonies (EryP) and macrophage/mixed colonies (Mac/Mixed) formed from day 5 populations induced as in Fig. 1. Colonies were scored following 7 days of culture in methylcellulose-based media containing hematopoietic cytokines. Error bars indicate s.e.m. (*n*=3). EB-derived cells were plated in 1% (w/v) methylcellulose containing 10% (v/v) plasma-derived serum, 5% (v/v) protein-free hybridoma medium (PFHM-II) and the following cytokines: 1% (v/v) kit ligand conditioned medium, 1% (v/v) thrombopoietin conditioned medium, erythropoietin (2 U/ml), IL11 (25 ng/ml), 1% (v/v) IL3 conditioned medium, 1% (v/v) GM-CSF conditioned medium and IL6 (5 ng/ml).

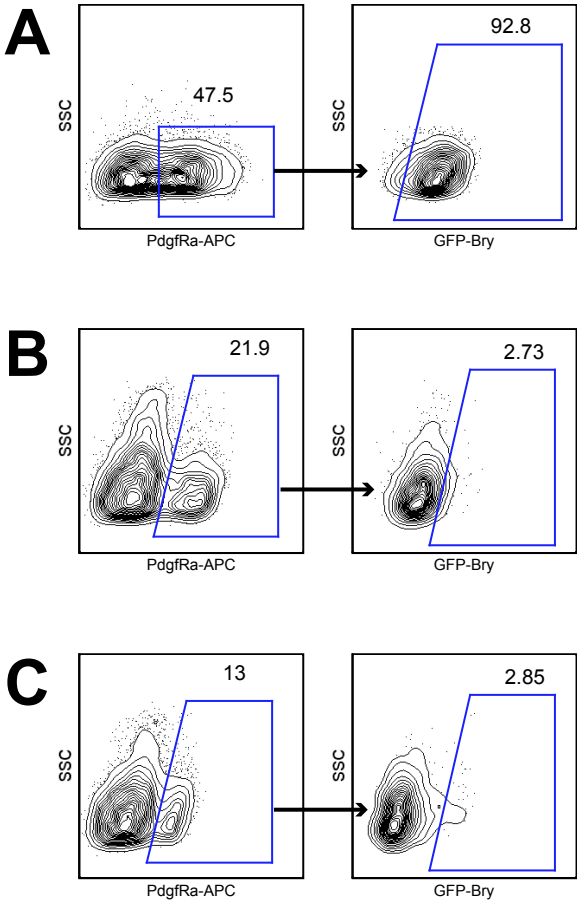

Fig. S3. Pdgfrα populations at day 3 and day 5 are distinguished by the expression of Brachyury. Populations were first gated on P^+ cells, expression of GFP-Bry was observed in P^+ cells. (**A**) The majority (>92%) of day 3 P^+ cells in noggin-induced EBs express GFP-Bry. (**B**,**C**) Less than 3% of day 5 P^+ cells derived from either day 3 P^- aggregates (B) or bulk (unsorted on day 3) aggregates (C) express GFP-Bry.

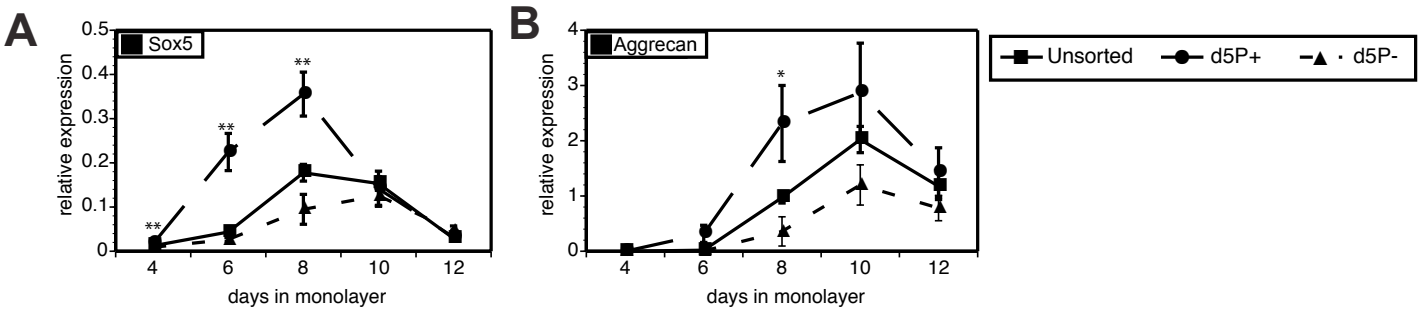

Fig. S4. Chondrogenic potential is detected in the Bry^{-}P^{+} cell fraction isolated from bulk differentiation cultures on day 5. (**A**,**B**) P^{+} and P^{-} populations were isolated by FACS from day 5 aggregates and cultured in monolayers in CH media for an additional 12 days. *Sox5* (A) and aggrecan (B) expression were significantly higher in d5P^{+}-derived monolayers compared with d5P^{-}-derived cultures. Significance of gene expression values in d5P^{+} monolayer cultures was compared with d5P^{-}-derived cultures. Error bars indicate s.e.m. (n=3). Values represent copy number relative to β-actin. *P<0.05, **P<0.01, ***P<0.001.

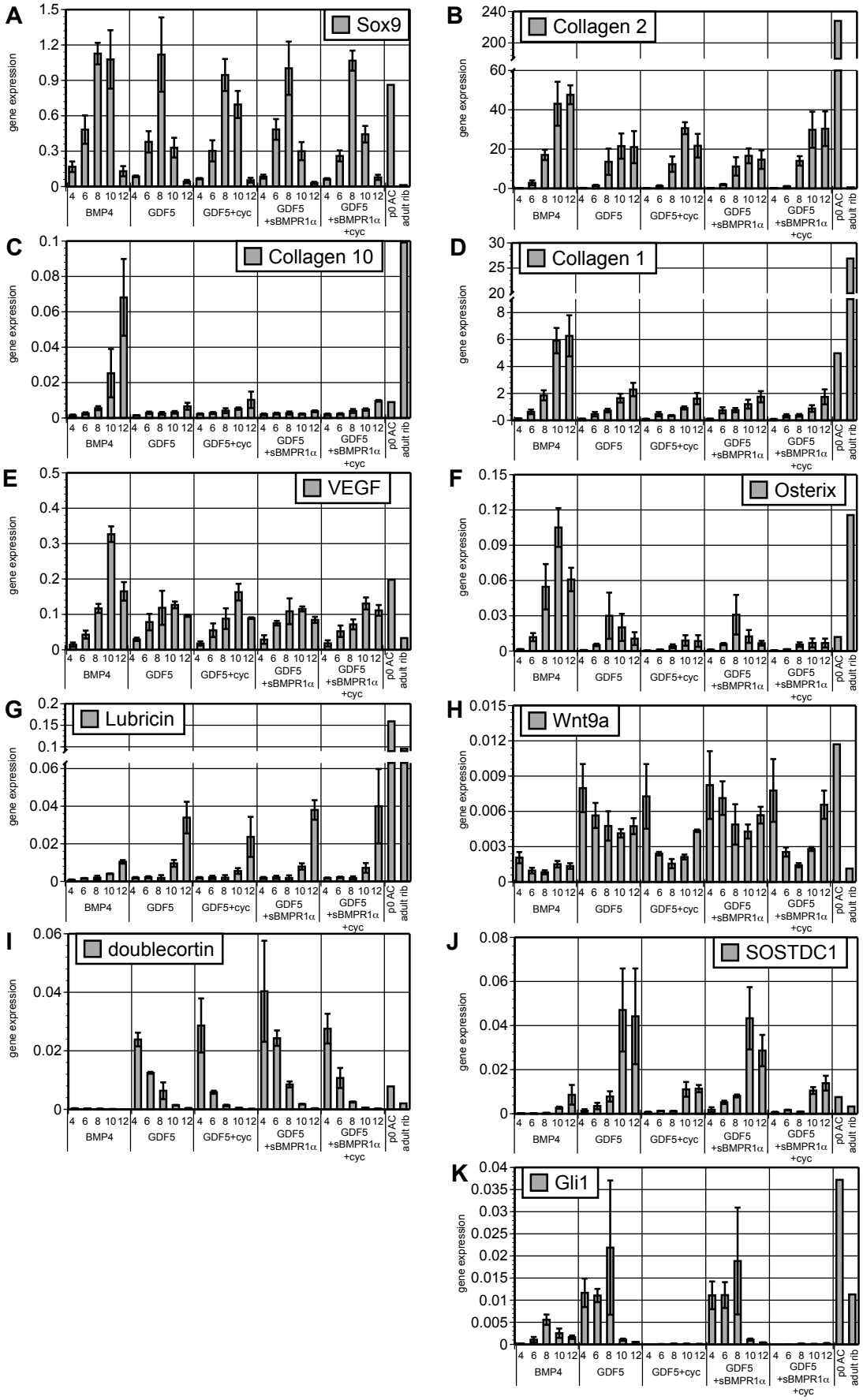

Fig. S5. Gene expression profiles of BMP4- and Gdf5-treated mESC-derived mesoderm in the presence of the BMP4 inhibitor sBmpr1α and the hedgehog inhibitor cyclopamine (cyc) during monolayer culture. (**A-K**) Gene expression analyses of the indicated genes following 4, 6, 8, 10 and 12 days of monolayer culture under different culture conditions. Values represent copy number relative to β-actin.

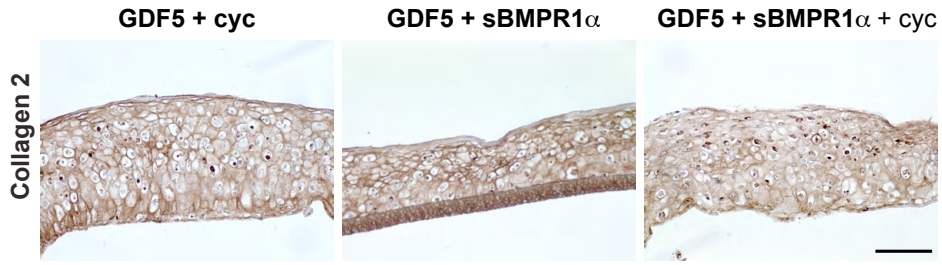

Fig. S6. Chondrocytes that develop in cultures with Gdf5, the hedgehog inhibitor (cyc) and/or the BMP4 inhibitor (sBmpr1α) generated cartilage-like tissues that express collagen 2. Filter cultures were analyzed after 5 weeks and immunohistochemistry was used to visualize collagen 2 expression. Scale bar: 100 μm.

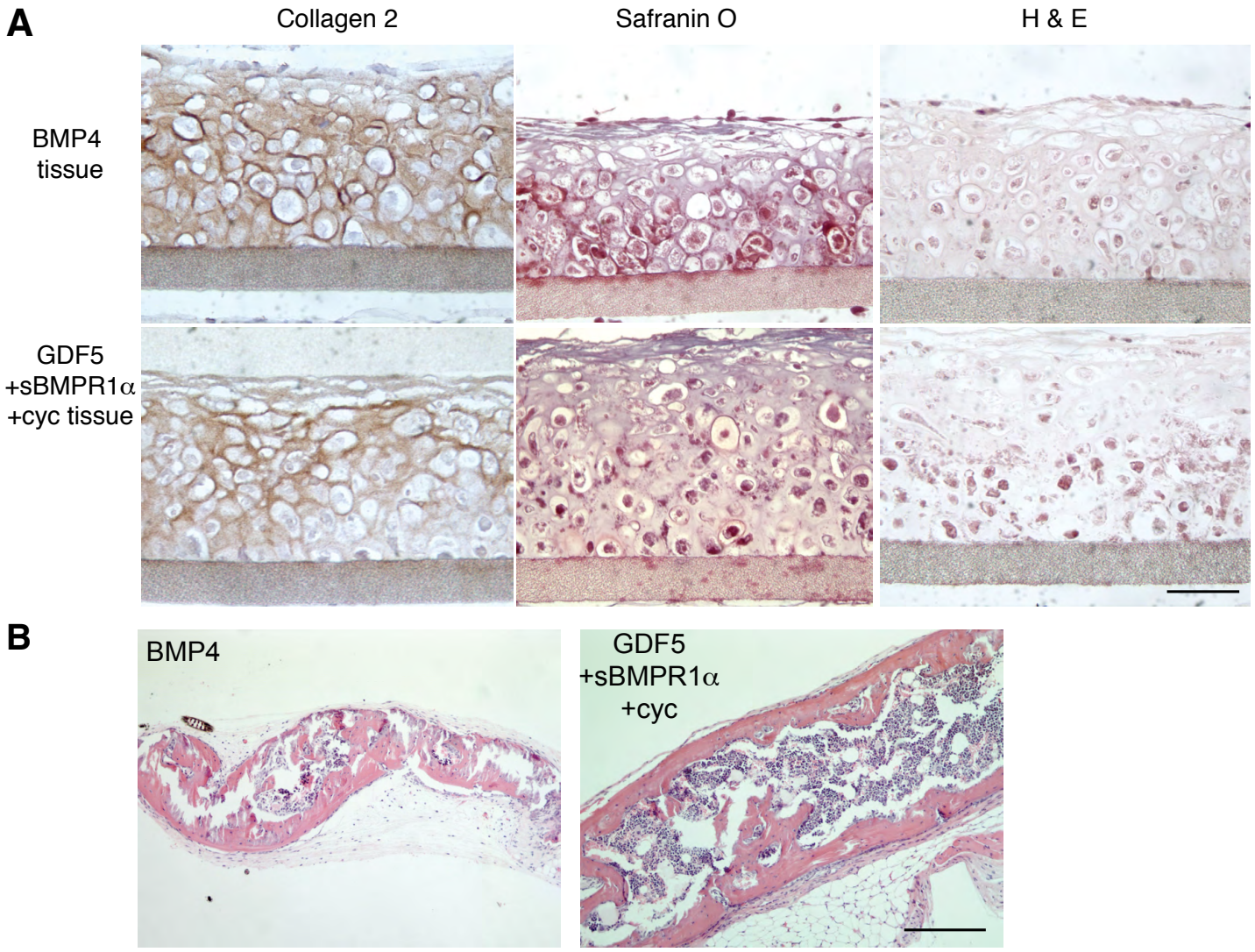

Fig. S7. Mouse ESC-derived cartilage tissue transplanted within diffusion chambers for 4 weeks shows no evidence of ossification, whereas comparable tissue transplanted without the chambers for the same period of time is completely ossified. Cartilage-like tissue was generated from BMP4-treated or Gdf5+sBmpr1α+cyc-treated chondrocytes for 4 weeks *in vitro* and then placed within diffusion chambers prior to subcutaneous implantation into immunodeficient mice. Mice were sacrificed at 4 weeks post transplantation, the diffusion chambers were isolated and the contents analyzed histologically for the presence of stable cartilage and/or bone-like tissue. (**A**) Collagen 2 immunohistochemistry, safranin O and Hematoxylin and Eosin (H&E) staining of cartilage-like tissue that was harvested after 4 weeks *in vivo*. (**B**) Three-dimensional cartilage tissue derived from mESCs were transplanted subcutaneously for 4 weeks. H&E staining of the grafts after 4 weeks shows bone-like tissue and hematopoietic cells contained within the graft. Scale bars: 50 in A; 100 μm in B.

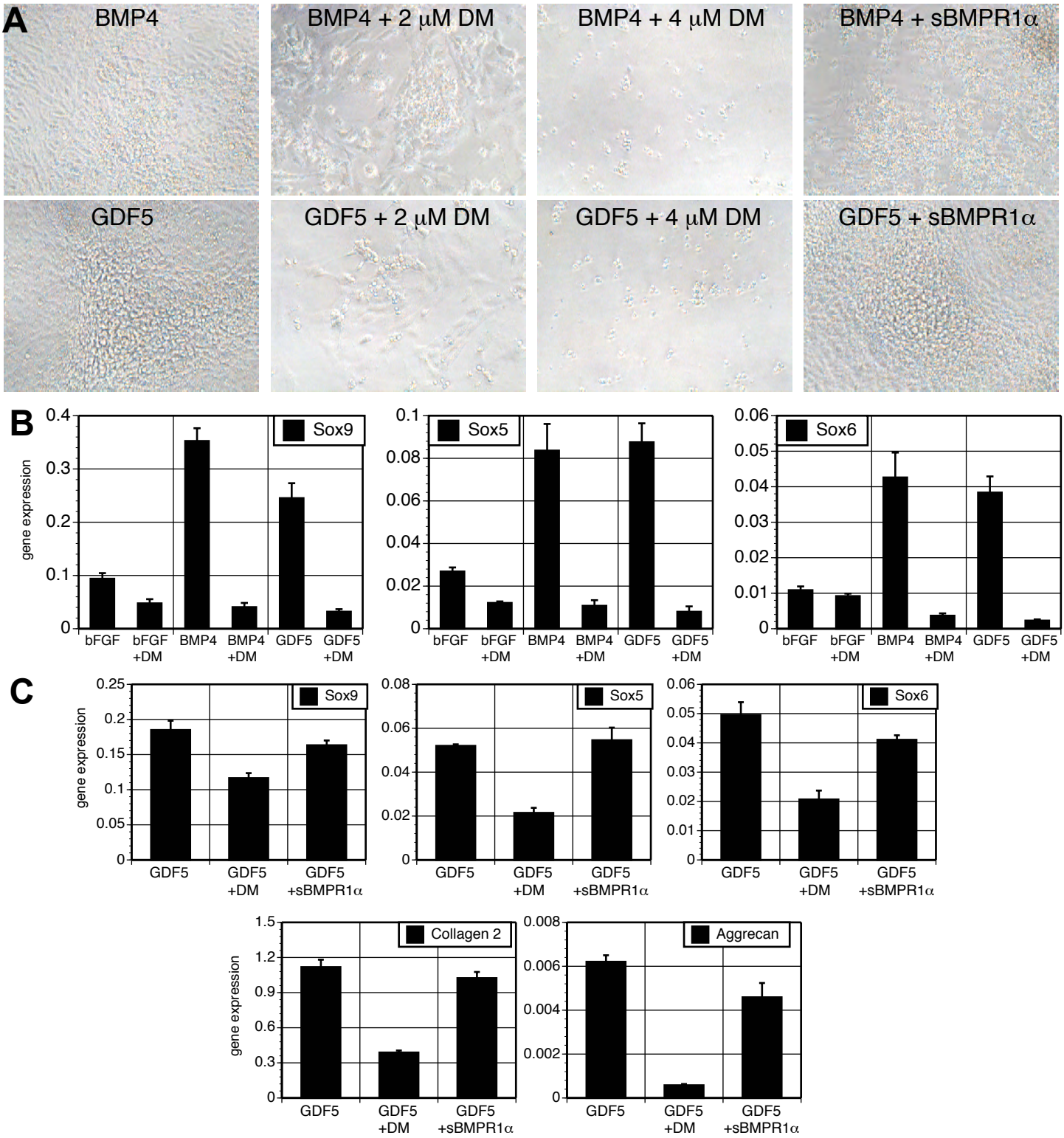

Fig. S8. BMP4 and Gdf5-mediated chondrogenic effects appear to be dependent on Bmpr1-mediated phosphorylation events. mESC-derived chondrogenic mesoderm was cultured in the presence of BMP4 or Gdf5 in combination with effective doses of dorsomorphin (DM), the small molecule inhibitor of the type I receptors Alk-2, -3, -6, or with the soluble Bmpr1α (sBmpr1α). (**A**) Micrographs of monolayer cultures in indicated conditions after 7 days. DM treatment at 4 μM resulted in cell death, whereas a lower concentration (2 μM) inhibited chondrogenesis in both BMP4- and Gdf5-treated cells. Gdf5-mediated chondrogenesis was not inhibited by sBmpr1α, whereas BMP4-mediated chondrogenesis was inhibited by sBmpr1α. Magnification 20×. (**B**) DM treatment (2 μM) prevented the upregulation of chondrocyte transcription factors *Sox9, Sox5* and *Sox6* in day 6 monolayers treated with BMP4 or Gdf5. (**C**) sBmpr1α did not prevent the expression of chondrogenic transcription factors or collagen 2 and aggrecan expression in Gdf5-treated cultures on day 7. Gene expression is copy number relative to β-actin.

Table S1. Primers

Gene	Forward	Reverse
β-actin	TGA GCG CAA GTA CTC TGT GTG GAT	ACT CAT CGT ACT CCT GCT TGC TGA
Tcf15	AAG GAC TCC AGA GAA AGA GGC CAT	TCC TTA CAC AAC GCA GGA GTG GTT
Meox1	AGC GTC TTG TGT TCT CCA AGG	ATG TGT GTG AAC CTG GGA GGT
Nkx3.2	TCA GAA CCG TCG CTA CAA GAC CAA	CAG CAC CTT TAC GGC CAC TTT CTT
Tbx18	CGC CCA GCC ATT CCT GTT TAT TCT	AAG GCT GTC ATC CAC CTT CCT TCA
Mesp1	TTT CCT TTG GTC TTG GCA CCT TCG	TCC AAG GAG GGT TGG AAT GGT ACA
Foxf1a	ATG CCA TGG CCT CTT CTT CTA TGC	ACA CGG CTT GAT GTC TTG GTA GGT
Gata1	ATG GAA TCC AGA CGA GGA	CTC CCC ACA ATT CCC ACT
Nkx2.5	ACC TTT AGG AGA AGG GCG ATG ACT	AAG TGG GAT GGA TCG GAG AAA GGT
Sox9	AGG TTT CAG ATG CAG TGA GGA GCA	CAC AAC ACA CGC ACA CAT CCA CAT
Sox5	ATA AGG GCC AAC AGA CTG TGG TGA	GTT AAT GTG CTT GGC CAC TGG GAA
Sox6	ATT CCT CCT CCA AGG CTG ACA ACA	GGC CAG CAT TTG ACA AGT GGA ACA
Col2a1	CCA AAC ACT TTC CAA CCG CAG TCA	AGT CTG CCC AGT TCA GGT CTC TTA
aggrecan	ATC CCA CCC ACA TGG TGT CTT CTT	TTA GAT GCA GTT TGG GTG ATG CGG
Col10a1	TGG AGA TGC ATT TGG AGG TAG GCT	AGG GCT TTA GGA TTG CTG AGT GCT
Col1a1	TGG CGG TTA TGA CTT CAG CTT CCT	GGT CAC GAA CCA CGT TAG CAT CAT’
0sterix	TTG CCA GTG CCT AGT TCC TAT GCT	AGG CCA GAT GGA AGC TGT GAA GAA
Vegf	GTG TGT GTG TGT GTG TGT GTG TGT	TCA CCG ATC TGG GAG AGA GAG ATT
lubricin	AGC CAA TGA AGA AGT GCA CAG GGA	AGG TGT GTG TCT GGA AAG GTC CAA
Wnt9a	AGG CCA GAG CCT CTT TGA TCT TCT	AAA GAC AGC TCC CTT GTG AGT CCA
doublecortin	GGA ATG TTT GGC AAG GCC CAT GTA	AGT CCT CAA ACC AAA CAG CCC TCA
Sostdc1	AGT CCA GCC ACA ACT TTG AAA GCG	AGA CTG TGC TTG CTG GAT TTG CTG
Gli1	ACA CTC AGC TGG ACT TTG TGG CTA	AGA CAC TCA TGT TAC CCA CTG CCA